

Short-term suppression of A315T mutant human TDP-43 expression improves functional deficits in a novel inducible transgenic mouse model of FTLD-TDP and ALS

Yazi D. Ke^{1,2} · Annika van Hummel^{1,2} · Claire H. Stevens¹ · Amadeus Gladbach¹ · Stefania Ippati¹ · Mian Bi¹ · Wei S. Lee¹ · Sarah Krüger¹ · Julia van der Hoven¹ · Alexander Volkerling¹ · Andre Bongers³ · Glenda Halliday⁴ · Nikolas K. Haass⁵ · Matthew Kiernan⁶ · Fabien Delerue^{1,7} · Lars M. Ittner^{1,4,7}

Received: 10 June 2015 / Revised: 26 September 2015 / Accepted: 27 September 2015 / Published online: 5 October 2015
© Springer-Verlag Berlin Heidelberg 2015

Abstract The nuclear transactive response DNA-binding protein 43 (TDP-43) undergoes relocalization to the cytoplasm with formation of cytoplasmic deposits in neurons in amyotrophic lateral sclerosis (ALS) and frontotemporal lobar degeneration (FTLD). Pathogenic mutations in the TDP-43-encoding *TARDBP* gene in familial ALS as well as non-mutant human TDP-43 have been utilized to model FTD/ALS in cell culture and animals, including mice. Here, we report novel A315T mutant TDP-43 transgenic mice, iTDP-43^{A315T}, with controlled neuronal over-expression. Constitutive expression of human TDP-43^{A315T} resulted in pronounced early-onset and progressive neurodegeneration, which was associated with compromised motor performance, spatial memory and disinhibition. Muscle atrophy resulted in reduced grip strength. Cortical degeneration presented with pronounced astrocyte activation. Using differential protein extraction from iTDP-43^{A315T} brains, we found cytoplasmic localization, fragmentation, phosphorylation and ubiquitination and insolubility of TDP-43. Surprisingly, suppression of human TDP-43^{A315T} expression

in mice with overt neurodegeneration for only 1 week was sufficient to significantly improve motor and behavioral deficits, and reduce astrogliosis. Our data suggest that functional deficits in iTDP-43^{A315T} mice are at least in part a direct and transient effect of the presence of TDP-43^{A315T}. Furthermore, it illustrates the compensatory capacity of compromised neurons once transgenic TDP-43 is removed, with implications for future treatments.

Keywords TDP-43 · Frontotemporal lobar degeneration · Amyotrophic lateral sclerosis · Mouse model · Pathogenic mutation

Introduction

Frontotemporal lobar degeneration (FTLD) and amyotrophic lateral sclerosis (ALS) are both incurable and rapidly progressive neurodegenerative diseases of the CNS, and represent a disease continuum with shared symptoms,

Y. D. Ke, A. van Hummel and C. H. Stevens contributed equally to this work.

Electronic supplementary material The online version of this article (doi:10.1007/s00401-015-1486-0) contains supplementary material, which is available to authorized users.

✉ Lars M. Ittner
l.ittner@unsw.edu.au

¹ Dementia Research Unit, Department of Anatomy, Faculty of Medicine, School of Medical Sciences, UNSW Australia, Sydney, NSW 2052, Australia

² Motor Neuron Disease Unit, Department of Anatomy, Faculty of Medicine, School of Medical Sciences, UNSW Australia, Sydney, NSW 2052, Australia

³ Biological Resources Imaging Laboratory, Mark Wainwright Analytical Centre, UNSW Australia, Sydney, NSW 2052, Australia

⁴ Neuroscience Research Australia, Sydney, NSW 2036, Australia

⁵ The University of Queensland Diamantina Institute, Translational Research Institute, The University of Queensland, Brisbane, QLD 4102, Australia

⁶ Brain and Mind Research Institute, Faculty of Medicine, Sydney Medical School, The University of Sydney, Sydney, NSW 2050, Australia

⁷ Transgenic Animal Unit, Mark Wainwright Analytical Centre, UNSW Australia, Sydney, NSW 2052, Australia

neuropathology and underlying genetics [24]. While muscle weakness is the predominant symptom of ALS, FTLN is characterized by behavioral and memory deficits [17]. Neuropathologically, both FTLN and ALS present with pathological deposition of ubiquitinated and aberrantly phosphorylated proteins in neurons and, less frequently, other CNS cell types [29]. At post-mortem examination, cytoplasmic deposits consisting of the nuclear TAR DNA-binding protein 43 (TDP-43) are found in a large proportion of FTLN (FTLN-TDP) and ALS brains [31]. In addition, up to 57 % of Alzheimer's disease (AD) brains show TDP-43 inclusions [27]. Interestingly, not only pathogenic mutations in the TDP-43-encoding gene *TARDBP*, identified in familial ALS [28, 40] result in nucleocytoplasmic re-localization and deposition of TDP-43, but also other familial FTLN-TDP and ALS-causing mutations lead to TDP-43 pathology. These include mutations in *GRN*, *C9ORF72* and other genes [2, 7, 9, 33]. Together, this suggests a central role of TDP-43 in the pathogenesis of FTLN-TDP, ALS and possibly other neurodegenerative diseases.

TDP-43 is a nuclear protein with two DNA/RNA binding domains followed by a glycine-rich domain, which is where virtually all pathogenic *TARDBP* mutations have been identified [28, 40]. Nuclear localization is regulated by nuclear localization and export sequences within the amino-terminal half of the protein [48]. The pathomechanism leading to nucleocytoplasmic re-localization of TDP-43 in FTLN-TDP and ALS remains unknown. Several physiological functions have been attributed to TDP-43, including RNA transport, alternative mRNA splicing and others [4], and loss of these functions may contribute to disease [43].

A range of transgenic TDP-43 expressing and *Tardbp*-deficient mouse lines have been generated to study the pathogenic role of TDP-43 in vivo [34]. Transgenic lines include constitutive expression of non-mutant and mutant TDP-43 under control of different promoters [45, 46], as well as the usage of inducible promoter systems [5, 8, 21]. Both approaches reproduced some neuropathological features of FTLN-TDP and ALS, and mice with inducible TDP-43 expression showed significant neuronal cell loss. While neuropathological changes have been examined in the latter models [5, 8, 21], the number of functional studies is low [24].

Here, we used a second-generation doxycycline-inducible system to express human TDP-43 carrying the pathogenic A315T mutation in CNS neurons in mice (iTDP-43^{A315T}). iTDP-43^{A315T} mice present with early functional deficits and pronounced neurodegeneration in the presence of a marked astrogliosis. Furthermore, we show beneficial effects of short-term suppression of TDP-43^{A315T} in mice after the onset of neurodegeneration.

Methods

Generation of iTDP-43^{A315T} mice

A cDNA encoding human TDP-43 was first cloned into pBluescript vector where the c.1077G>A nucleotide exchange that results in an A315T amino acid switch was introduced by site-directed mutagenesis using previously reported protocols [26]. Correct mutagenesis was confirmed by sequencing. The A315T-hTDP43 encoding cDNA was then excised with *Bam*HI and *Xba*I and cloned into the *Bam*HI and *Xba*I sites of the pTRE-tight vector (Clontech, USA). A fragment containing the pTRE-tight promoter, A315T-hTDP-43 cDNA and a SV40 poly A sequence was obtained via *Xho*I digestion and purified for pronuclear injection. The fragment was injected into fertilized C57Bl/6 oocytes for the generation of transgenic mice [23]. Five founders were identified by PCR, using the following primer pair: 5'-ccgatggtatttcaatggct-3' and 5'-agagaacgatgtcgcaggtagg-3'. Four founders transmitted the transgene to their offspring and four lines showed expression of hTDP-43 when crossed with a TetOFF line. We selected 2 lines, pTRE-TDP-43^{A315T}(6) and pTRE-TDP-43^{A315T}(13), with comparable expression levels for further analysis. mThy1.2-tTA(6) and mThy1.2-tTA(15) mice have previously been published by us [10]. Littermates were used as controls throughout this study. TDP-43 expressing mice were compared to both non-transgenic (wild type) and single transgenic (mThy1.2-tTA(6), mThy1.2-tTA(15), pTRE-TDP-43^{A315T}(6) or pTRE-TDP-43^{A315T}(13)) controls. Mice of both sexes were used throughout the study, showing no gender differences in phenotypes. All animal experiments have been approved by the Animal Care and Ethics Committee of the University of New South Wales.

Doxycycline treatment

To suppress transgene expression, mice received doxycycline 1 week prior to commencement of behavioral tests and throughout the testing period. Doxycycline was added to the standard diet (Cat No. SF11-059; Specialty Feeds, Glen Forrest, Australia) at a concentration of 200 mg/kg, as previously reported by others and us [10].

Histological analysis

Mice were anesthetized and transcardially perfused with phosphate buffered saline. Brains, spinal cords and calf muscles were removed and the hemispheres separated. One hemisphere of the brain was immersion-fixed in 4 % paraformaldehyde for immunohistochemical analysis, and the other hemisphere was sub-dissected and snap-frozen in

liquid nitrogen for biochemical analysis. Fixed brains were processed using an automated system (Excelsior, Thermo, USA), embedded in paraffin and sagittally sectioned at the level of the mid-hippocampus into 3- μm -thick sections using a microtome (Thermo, USA). All staining was done in Sequenza staining racks for standardization using previously reported protocols [41]. The following primary antibodies were used: human TDP-43 (60019-2-Ig, Proteintech), mouse TDP-43 (Gift by Prof Virginia Lee [21]), pan-TDP-43 (10782-2-AP, Proteintech), laminin (L9393, Sigma), POU3F2 (ab94977, Abcam), ubiquitin (MAB1510, Millipore), GFAP (G9269 Sigma), IBA-1 (019-19741, Wako). Microscopy was performed with an Olympus BX51 (USA) epi-fluorescence microscope equipped with a DP70 color camera, or sections were scanned with an Aperio Scanscope (USA). Quantification was done on serial sections using landmark structures as guides as described [42]. Alpha-motor neurons were counted on 3 serial cross sections (covering 150 μm) each at 3 levels of spinal cords. The total number of human-specific TDP-43-positive cells was counted throughout the sub-regions of the hippocampus. For the cortex, two representative images of the pathology in layers II/III and layer V immediately adjacent to the hippocampus were taken at 400 \times magnification and the number of positive cells counted. Similarly, GFAP-positive astrocytes and POU3F2-positive layer V neurons were counted in the cortex. Olympus CellSens software was used to delineate the regions of interest, and area and width measurements automatically calculated. The width of the cortex was determined immediately adjacent to the hippocampus. All cell counts were converted to density values (cells/ μm^2). Muscle fibers were delineated via laminin immunoreaction and cross-sectional area quantified via a semi-automated approach in ImageJ (NIH). Density distribution curves were generated via kernel density estimation function in RStudio.

Sequential extraction and Western blotting

Using 50–100 mg of tissue for each region, proteins were extracted according to solubility as previously described [48], into either a modified RIPA buffer (50 mM Tris-HCl (pH 8), 150 mM NaCl, 1 % Triton X, 0.5 % Na-deoxycholate, 1 % sodium dodecyl sulfate, 3 mM EDTA and protease inhibitor (Roche)) or UREA buffer (7 M UREA, 2 M thiourea, 4 % Chaps 3 mM Tris, pH 8.5). The protein concentration of each sample was determined using the Bradford assay (BioRad). Sequential extraction of nuclear and cytosolic proteins was carried out as previously described [13]. Protein extracts were analyzed by immunoblotting, as previously described [25]. Briefly, between 15 and 60 μg of total protein were loaded and separated on 8–10 % SDS-PAGE gels. Proteins were then electrophoretically

transferred onto nitrocellulose membranes (Hybond). These membranes were blocked with bovine serum albumin and incubated overnight with primary antibodies, pan-TDP-43, human TDP-43 (Proteintech), ubiquitin or GAPDH (Millipore). Horseradish peroxidase-coupled secondary antibodies were used and protein bands were visualized using Luminata Crescendo Western HRP Substrate (Millipore) and detected using the ChemiDoc MP System (BioRad).

Behavioral, memory and motor testing

Rota-Rod

Motor performance of mice was determined using a Rota-Rod (Ugo Basile) in acceleration mode (5–60 rpm) over 120 s. The longest time each mouse remained on the turning wheel out of 5 attempts per session was recorded.

Elevated Plus maze

The Elevated Plus maze (Ugo Basile) consisted of two open and two closed arms (each 35 cm \times 5.5 cm), as well as a central platform (5.5 cm \times 5.5 cm), elevated 60 cm above the ground. Mice were acclimatized to the room for 1 h prior to testing, then placed on the center platform facing an open arm and recorded for 5 min. Videos were analyzed using the AnyMaze software.

Open field

Mice were placed at the periphery of a 40 cm \times 40 cm Perspex box in an enclosed cupboard and videoed for 10 min. Videos were analyzed using the AnyMaze software, and the box divided into an outer and inner zone (inner zone was a 17.5 cm \times 17.5 cm square in the center of the box).

Pole test

To test strength and coordination, mice were placed at the apex of a vertical pole (47.5 cm length of dowel, diameter 0.8 cm) facing upwards. The time taken to turn around, descend the pole and reach the ground (with all four paws) was measured with a maximum time of 120 s. Mice underwent 1–2 training sessions prior to the test session, during which the average time was taken out of three trials. Mice that were unable to descend the pole (slipped or fell) were given the maximum time.

Morris water maze

The apparatus consisted of a 1.2-m-diameter tank with a 40-cm-high Perspex platform (diameter 10 cm), which was placed roughly 20 cm from the edge of the wall. The

tank was filled to 0.5–1 cm above the surface of the platform and a non-toxic, acrylic-based paint was added to the water to obscure the platform. Four signposts with different shapes were placed equidistant around the pool as visual cues. Mice were acclimatized to the room for 1 h prior to testing each day. Days 1–5 consisted of an acquisition phase, in which mice were placed in the quadrant opposite the platform at one of four starting positions and given 60 s to locate the hidden platform. Mice that failed to find the hidden platform were guided to the escape platform and all mice remained on the platform for an additional 60 s before being removed from the maze. Mice had four trials per day, each starting from a different position, and the order of starting positions was altered each day. On the sixth day, the platform was removed and the mice were given 30 s to explore the pool (probe trial). On the seventh day, the platform was placed back in the pool with a flag attached, and visual cues were removed from outside of the pool, to ensure that all mice had normal vision. Videos were analyzed using the AnyMaze software.

Grip strength test

A grip strength meter (Chatillon, AMETEK) was used to measure the force exerted by the forelimbs of the mouse as it was pulled away from a thin metal wire by the tail. Mice were placed such that they had a double grip on a thin metal wire attached to the meter, and they were pulled away from the meter in a horizontal direction until they let go, and a peak force (N) was recorded at the moment when the mice let go. The highest force from three attempts was recorded.

Magnetic resonance imaging (MRI)

Mice were anesthetized and transcardially perfused with phosphate buffered saline followed by cold 4 % paraformaldehyde (PFA). Brains and tissues were removed and post-fixed in 4 % PFA over night. Prior to imaging the fixed brains were immersed in 0.2 % v/v Gd-DTPA + 9 g/l NaCl/H₂O solution for 24–48 h at 21 °C to reduce T1 relaxation time of the brain tissue. The brains were then transferred into a 1.3 mm ID, 2 ml Cryovial (Greiner, Germany) and submersed in Perfluoro-Polyether Fomblin™ 6Y for susceptibility matching. The Cryovial was then mounted on the tip of a plastic tube, which was attached to the automatic positioning system of the MRI system. High-resolution anatomical imaging of the brain samples was performed in a 9.4-T Bruker BioSpec 94/20 Avance III micro-imaging system (Bruker, Ettlingen, Germany) which was equipped with BGA-12S HP gradients with maximum strength 660 mT/m and slew rate 4570 Tm/s and

a dedicated 15 mm Quadrature Receive/Transmit RF-coil (Bruker, Ettlingen, Germany) to optimize MR signal.

For image acquisition, an optimized, isotropic 3D Fast Low Angle Shot (FLASH) pulse sequence protocol in coronal slice orientation was used with the following major parameters: TE = 6 ms, TR = 100 ms, FA = 40°, FOV = 15 × 15 × 8 mm, matrix = 200 × 200 × 106, Image Resolution = 75 μm³ (isotropic), Eff. Spectral BW = 51,020 Hz, Total acquisition time with 2 ADC averages: 1 h and 10 min per specimen. Total brain volume and hippocampal volume and segmentation were obtained using 3D Slicer software (NIH).

Statistical analysis

All statistical analysis was done using the Graphpad Prism 6.0 software at Student's *t* test and ANOVA (Bonferroni's multiple comparison test). *P* values of below 0.05 were considered significant. All values are presented as mean and standard error of the mean.

Results

A315T mutant human TDP-43 expression in mice

To study the effects of mutant TDP-43 in vivo, we generated novel transgenic mouse lines with inducible expression of human TDP-43 carrying the pathogenic A315T mutation found in familial ALS. The c.1077G>A mutation was introduced into human TDP-43-encoding cDNA by site-directed mutagenesis. Mutant TDP-43^{A315T} was then cloned into a second-generation tetracycline-responsive element promoter plasmid (pTRE-tight) for pronuclear injection into C57Bl/6 oocytes [23]. Transgenic F0 offspring were identified by PCR and crossed with mThy1.2-tTA transgenic mice, which drive constitutive expression from pTRE-tight in neurons, to establish inducible iTDP-43^{A315T} lines (Fig. 1a). Four out of five independent TDP-43^{A315T} lines showed expression of human TDP-43 in the brain. The two lines, pTRE-TDP-43^{A315T}(6) and pTRE-TDP-43^{A315T}(13), were selected for further analysis due to similar high expression levels when crossed on the same mThy1.2-tTA lines (Fig. 1b) and Mendelian inheritance of the transgene was maintained across generations. To establish iTDP-43^{A315T} expressing lines, both pTRE-TDP-43^{A315T}(6) and pTRE-TDP-43^{A315T}(13) were crossed individually with two mThy1.2-tTA lines, mThy1.2-tTA(6) and mThy1.2-tTA(15), which differ slightly in pattern and levels of tetR expression [10]. Survival was not affected in iTDP-43^{A315T} lines. Expression levels of human TDP-43^{A315T} were first assessed by

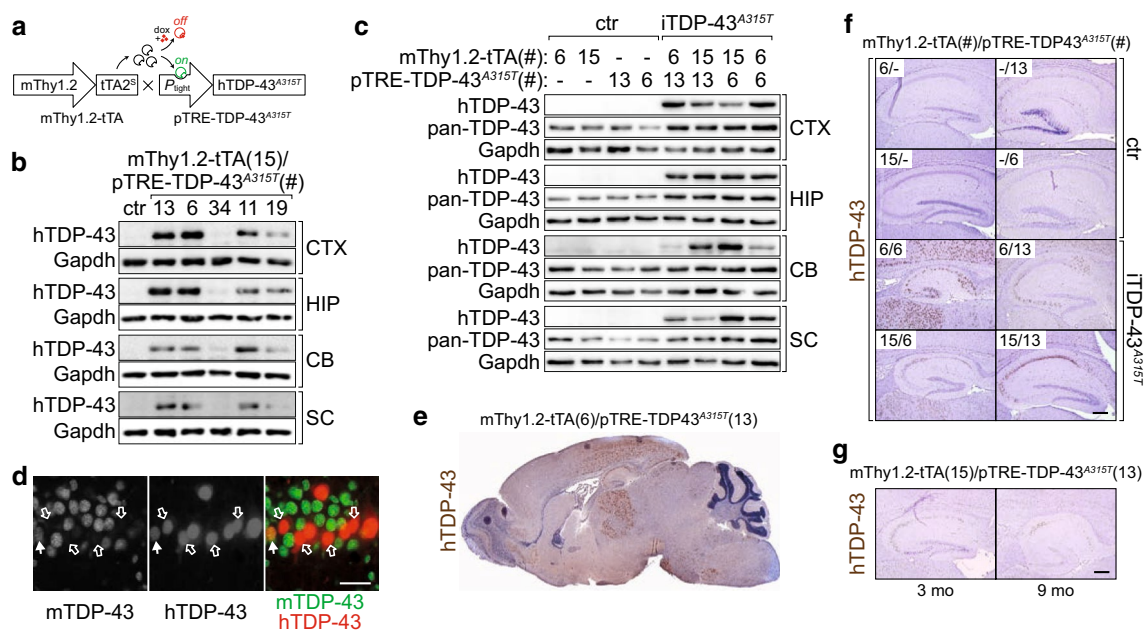


Fig. 1 Transgenic expression of TDP-43^{A315T} in neurons with early-onset hippocampal atrophy. **a** Transgenic mice with inducible expression of TDP-43^{A315T} in neurons (iTDP-43^{A315T}) were generated by crossing neuronal inducer lines mThy1.2-tTA with mouse strains harboring a TDP-43^{A315T} transgene under the control of the tetracycline-responsive promoter (pTRE-TDP-43^{A315T}). tTA binds and activates constitutive transgene expression in neurons (on). tTA binding to pTRE is blocked in the presence of doxycycline (dox) and transcription is switched off. **b** 5 pTRE-TDP-43^{A315T} founder lines (13, 6, 34, 11, 19) were crossed on mThy1.2-tTA(15) mice to select lines with similar expression levels, in cortex (CTX), hippocampus (HIP), cerebellum (CB) and spinal cord (SC), as determined by Western blotting. Lines 13 and 6 were continued. Detection of Gapdh confirmed equal loading. ctr = control. **c** Four different iTDP-43^{A315T} lines were established by crossing pTRE-TDP-43^{A315T}(6) and pTRE-TDP-43^{A315T}(13) mice with two different inducer lines, mThy1.2-tTA(6) and mThy1.2-tTA(15). Differences in human TDP-43^{A315T} expression levels in CTX, HIP, CB and SC were determined Western blotting with human TDP-43-specific antibodies (hTDP-43). Total TDP-43 levels in the 4 iTDP-43^{A315T} lines were compared to single transgenic pTRE-TDP-43^{A315T}(6), pTRE-TDP-43^{A315T}(13), mThy1.2-tTA(6) and mThy1.2-tTA(15) mice, using antibodies that detect both human and mouse TDP-43 (pan-TDP-43). Detection of Gapdh confirmed equal

loading. **d** Double immunofluorescence staining with an antibody specific to human (hTDP-43, red) and one specific to mouse TDP-43 (mTDP-43, green) was, apart from rare cells with double labeling (closed arrow), predominantly mutually exclusive (open arrows), suggesting down-regulation of mTDP-43 in human TDP-43^{A315T}-expressing cells. While mTDP-43 staining was purely nuclear, some hTDP-43 was found in the cytoplasm in addition to a strong nuclear signal. Scale bar 50 μ m. **e** Scan of a full sagittal brain section from a mThy1.2-tTA(6)/pTRE-TDP-43^{A315T}(13) mouse stained with hTDP-43 (brown) illustrated the transgene expression pattern in different brain areas. **f** Comparison of matched sagittal hippocampal sections from all 4 different iTDP-43^{A315T} lines and the corresponding single transgenic controls at 1 month of age, stained for human TDP-43^{A315T} (hTDP-43, brown). Line combinations are indicated in each panel. Hippocampal sizes were most evidently reduced in mThy1.2-tTA(6)/pTRE-TDP-43^{A315T}(6) followed by mThy1.2-tTA(15)/pTRE-TDP-43^{A315T}(6) and mThy1.2-tTA(6)/pTRE-TDP-43^{A315T}(13) mice. The hippocampus in mThy1.2-tTA(15)/pTRE-TDP-43^{A315T}(13) mice was nearly normal sized. Scale bar, 250 μ m. **g** Eventually, the hippocampus of mThy1.2-tTA(15)/pTRE-TDP-43^{A315T}(13) mice became also atrophic at 3 and more so at 9 months of age, indicating slower progression of neuronal loss compared to the other iTDP-43^{A315T} lines. Scale bar 250 μ m

Western blotting in extracts from hippocampus, cortex, cerebellum and spinal cords of all four iTDP-43^{A315T} lines [mThy1.2-tTA(6)/pTRE-TDP-43^{A315T}(6), mThy1.2-tTA(6)/pTRE-TDP-43^{A315T}(13), mThy1.2-tTA(15)/pTRE-TDP-43^{A315T}(6) and mThy1.2-tTA(15)/pTRE-TDP-43^{A315T}(13)] and single transgenic mThy1.2-tTA(6), mThy1.2-tTA(15), pTRE-TDP-43^{A315T}(6) and pTRE-TDP-43^{A315T}(13) mice at 4 weeks of age (Fig. 1c). Expression levels in the hippocampus were comparable in all four iTDP-43^{A315T} lines, with 2.0- to 2.1-fold increased TDP-43 levels compared to controls. mThy1.2-tTA(6)-driven TDP-43^{A315T} expression was slightly higher in the cortex of mThy1.2-tTA(6)/pTRE-TDP-43^{A315T}(6) (2.5-fold increased TDP-43 levels)

compared to mThy1.2-tTA(6)/pTRE-TDP-43^{A315T}(13), mThy1.2-tTA(15)/pTRE-TDP-43^{A315T}(6) and mThy1.2-tTA(15)/pTRE-TDP-43^{A315T}(13) mice (1.6- to 1.8-fold increased TDP-43 levels). Expression levels in spinal cords were lowest in mThy1.2-tTA(15)/pTRE-TDP-43^{A315T}(13) and mThy1.2-tTA(6)/pTRE-TDP-43^{A315T}(13) mice [1.5- to 1.7-fold increased TDP-43 levels, compared to 2.2-fold in mThy1.2-tTA(15)/pTRE-TDP-43^{A315T}(6) and 2.7-fold in mThy1.2-tTA(6)/pTRE-TDP-43^{A315T}(6)], and only mThy1.2-tTA(15)/pTRE-TDP-43^{A315T}(6) and mThy1.2-tTA(15)/pTRE-TDP-43^{A315T}(13) showed some TDP-43^{A315T} expression in the cerebellum (1.2- to 1.4-fold increased TDP-43 levels). No human TDP-43 was detected

in pTRE-TDP-43^{A315T}(6) and pTRE-TDP-43^{A315T}(13) extracts suggesting absence of leaky expression. Detection of pan-TDP-43 (=human TDP-43^{A315T} plus endogenous murine TDP-43) showed increased total levels of TDP-43 in all brain regions (Fig. 1c), while at the individual neuronal level immunofluorescence staining revealed a compensatory down-regulation of endogenous murine TDP-43 in the presence of transgenic human TDP-43^{A315T} (Fig. 1d), consistent with previous reports [21].

Next, we determined the expression pattern of transgenic TDP-43^{A315T} in all four lines by immunohistochemistry (IHC). Consistent with pan-neuronal tetR expression in mThy1.2-tTA mice [10], all four iTDP-43^{A315T} lines expressed transgenic TDP-43 in neurons throughout the brain, including all neuronal layers of the cortex, neurons of the CA1-3 region and dentate gyrus of the hippocampus, and spinal cord (Fig. 1e and data not shown). Most importantly, already at 4 weeks of age three of the four iTDP-43^{A315T} lines presented with much reduced hippocampal sizes, compared to monogenic littermate controls (Fig. 1f). This degeneration of the hippocampus was most severe in mThy1.2-tTA(6)/pTRE-TDP-43^{A315T}(6) mice and intermediate in mThy1.2-tTA(6)/pTRE-TDP-43^{A315T}(13) and mThy1.2-tTA(15)/pTRE-TDP-43^{A315T}(6) animals, while the mThy1.2-tTA(15)/pTRE-TDP-43^{A315T}(13) showed no overt alteration at 4 weeks of age. The latter line eventually presented with hippocampal degeneration, in particular of the CA1 region, in subsequent months (Fig. 1g). Taken together, we have generated new iTDP-43^{A315T} transgenic lines with neuronal expression and degeneration.

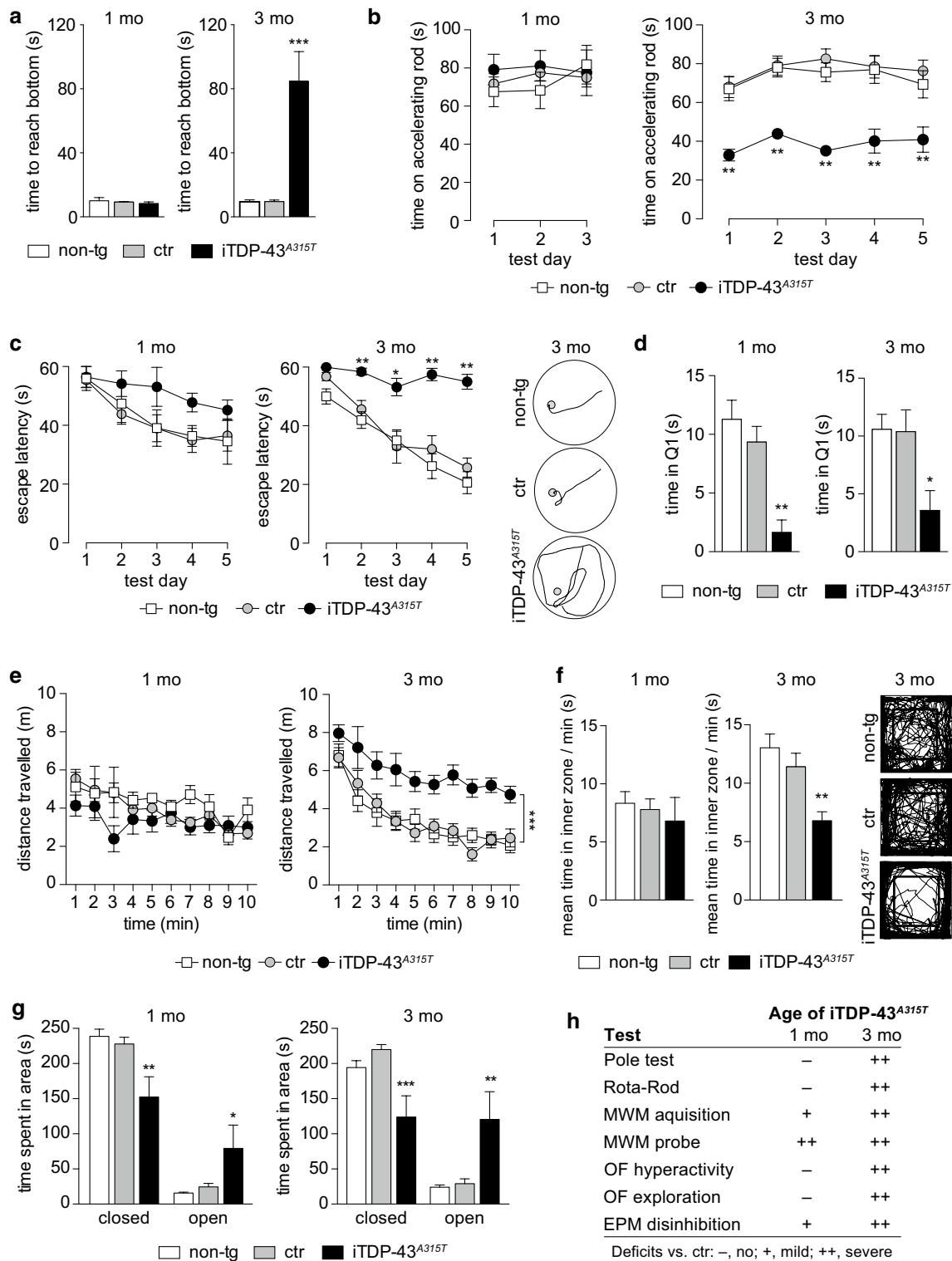
Functional deficits in iTDP-43^{A315T} mice

Next, we determined if transgenic TDP-43^{A315T} expression in CNS neurons compromised neuronal function, resulting in behavioral anomalies and impaired motor performance. To assess motor performance, we first subjected 1- and 3-month-old mThy1.2-tTA(6)/pTRE-TDP-43^{A315T}(13), single transgenic pTRE-TDP-43^{A315T}(13) and mThy1.2-tTA(6) control, and non-transgenic mice to the pole test paradigm (Fig. 2a). While 1-month-old mice showed no deficits, 3-month-old mThy1.2-tTA(6)/pTRE-TDP-43^{A315T}(13) mice showed a significant delay in turning at the top and reaching the bottom of a vertical pole, compared to non-transgenic and single transgenic pTRE-TDP-43^{A315T}(13) and mThy1.2-tTA control mice, suggesting compromised motor coordination. Three-month-old mThy1.2-tTA(15)/pTRE-TDP-43^{A315T}(13) displayed similar motor impairments during pole testing (Supplementary Fig. 1). For the subsequent detailed analysis of functional and morphological changes we focused on the mThy1.2-tTA(6)/pTRE-TDP-43^{A315T}(13) line, referred to as iTDP-43^{A315T}. Three, but not 1-month-old human TDP-43^{A315T}-expressing mice presented with a

Fig. 2 Motor, memory and behavioral deficits in iTDP-43^{A315T} mice. **a** Vertical pole test: while the performance of 1-month-old mThy1.2-tTA(6)/pTRE-TDP-43^{A315T}(13) iTDP-43^{A315T} mice was indistinguishable from single transgenic pTRE-TDP-43^{A315T}(6) and pTRE-TDP-43^{A315T}(13) controls (ctr), and non-transgenic (non-tg) mice [$n = 4$ (non-tg), $n = 14$ (ctr), $n = 6$ (iTDP-43^{A315T})], 3-month-old iTDP-43^{A315T} mice required significantly more time to reach the bottom when placed at the top of the pole, as compared to ctr and non-tg mice [***, $P < 0.001$, $n = 14$ (non-tg), $n = 20$ (ctr), $n = 7$ (iTDP-43^{A315T})]. **b** Accelerating Rota-Rod: iTDP-43^{A315T}, ctr and non-tg mice performed similarly at 1 month of age, but 3-month-old iTDP-43^{A315T} mice fell off the rotating rod much earlier than ctr and non-tg mice [**, $P < 0.01$, $n = 13$ (non-tg), $n = 14$ (ctr), $n = 8$ (iTDP-43^{A315T})]. **c** Morris water maze: already at 1 month of age memory acquisition was delayed in iTDP-43^{A315T} compared to ctr and non-tg mice [$n = 4$ (non-tg), $n = 14$ (ctr), $n = 6$ (iTDP-43^{A315T})], and 3-month-old iTDP-43^{A315T} mice were virtually unable to find the submerged escape platform, whereas ctr and non-tg mice presented with normal memory acquisition [**, $P < 0.01$, $n = 13$ (non-tg), $n = 14$ (ctr), $n = 8$ (iTDP-43^{A315T})]. Typical swimming traces at test day 5 are shown for 3-month-old mice. **d** Furthermore, iTDP-43^{A315T} mice spent significantly less time in the target quadrant (Q1) during probe trials, compared to ctr and non-tg mice [**, $P < 0.01$, 1 month: $n = 4$ (non-tg), $n = 14$ (ctr), $n = 6$ (iTDP-43^{A315T}), 3 months: $n = 13$ (non-tg), $n = 14$ (ctr), $n = 8$ (iTDP-43^{A315T})]. **e** Open field: while 1-month-old iTDP-43^{A315T}, ctr and non-tg mice were similarly active [$n = 4$ (non-tg), $n = 14$ (ctr), $n = 6$ (iTDP-43^{A315T})], 3-month-old iTDP-43^{A315T} mice travelled significantly more over 10 min in the open field arena compared to ctr and non-tg mice, suggesting hyperactivity [***, $P < 0.001$, $n = 13$ (non-tg), $n = 14$ (ctr), $n = 9$ (iTDP-43^{A315T})]. **f** At the same time, 3-month-old iTDP-43^{A315T} mice explored predominantly the periphery of the open field arena and spent significantly less time in the center compared to ctr and non-tg mice [**, $P < 0.01$, $n = 13$ (non-tg), $n = 14$ (ctr), $n = 9$ (iTDP-43^{A315T})]. Typical traces over 10 min are shown for 3-month-old mice. Exploration patterns of 1-month-old iTDP-43^{A315T}, ctr and non-tg mice were indistinguishable [$n = 4$ (non-tg), $n = 14$ (ctr), $n = 6$ (iTDP-43^{A315T})]. **g** Elevated plus maze: one, but more so 3-month-old mThy1.2-tTA(6)/pTRE-TDP-43^{A315T}(13) iTDP-43^{A315T} mice spent significantly less time in the closed and more time in the open arms of the EPM compared to single transgenic pTRE-TDP-43^{A315T}(6) and pTRE-TDP-43^{A315T}(13) controls (ctr), and non-transgenic mice, suggesting reduced anxiety and/or disinhibition [*, $P < 0.05$, **, $P < 0.01$, ***, $P < 0.001$, 1 month: $n = 4$ (non-tg), $n = 14$ (ctr), $n = 6$ (iTDP-43^{A315T}), 3 months: $n = 13$ (non-tg), $n = 14$ (ctr), $n = 8$ (iTDP-43^{A315T})]. **h** Summary of behavioral, memory and motor deficits in iTDP-43^{A315T} mice presented at 1 and 3 months of age

significantly reduced latency to fall off the rotating rod during accelerating-mode Rota-Rod testing, further supporting progressively impaired motor performance in iTDP-43^{A315T} transgenic mice (Fig. 2b). For comparison 1-month-old iTDP-43^{A315T}, and 1- and 3-month-old non-transgenic and single transgenic pTRE-TDP-43^{A315T}(13) and mThy1.2-tTA(6) control mice showed a similar latency to fall.

To determine if memory formation in iTDP-43^{A315T} mice is compromised, we assessed their spatial memory abilities using the Morris water maze paradigm. Decreasing latency to escape onto the submerged hidden platform over five consecutive testing days suggests normal memory formation in non-transgenic and single transgenic pTRE-TDP-43^{A315T}(13) and mThy1.2-tTA(6) control mice at 1



and 3 month of age (Fig. 2c). In contrast, already 1-month-old iTDP-43^{A315T} mice showed a delay in memory acquisition, and 3-month-old iTDP-43^{A315T} mice completely failed to learn, with mice only rarely finding the hidden platform even after 5 days despite being guided to the platform at

the end of each acquisition trial. During probe trials, iTDP-43^{A315T} mice spent much less time in the target quadrant than control mice, further supporting significantly compromised memory functions (Fig. 2d). Swim path length during the probe trials was comparable for 1-month-old

mice [5.6 ± 0.3 m (non-tg), 5.0 ± 0.3 m (ctr), 4.7 ± 0.7 m (iTDP-43^{A315T})], and only slightly reduced for 3-month-old iTDP-43^{A315T} mice [7.1 ± 0.1 m (non-tg), 6.9 ± 0.2 m (ctr), 4.4 ± 0.5 m (iTDP-43^{A315T})], suggesting that the observed deficits were indeed due to memory rather than motor deficits. Furthermore, all mice found the platform rapidly when it was equipped with a flag, suggesting normal vision and the ability to swim directly to a cued goal in iTDP-43^{A315T} and control mice.

When exposed to a novel environment in the open field arena, 3-month-old, but not 1-month-old iTDP-43^{A315T} mice presented with significantly increased distance travelled and hence higher speed compared to non-transgenic and single transgenic pTRE-TDP-43^{A315T}(13) and mThy1.2-tTA(6) control littermates (Fig. 2e). Furthermore, the exploration pattern of the open field arena differed markedly between 3-month-old iTDP-43^{A315T} and control mice (Fig. 2f). While 3-month-old control mice explored the whole arena during the 10-min test period, iTDP-43^{A315T} mice remained close to the edges of the arena at virtually all times. Exploration patterns of 1-month-old iTDP-43^{A315T} and control mice were indistinguishable (Fig. 2f). Hence, despite progressively reduced motor coordination, iTDP-43^{A315T} mice developed increased activity together with a compromised exploration strategy over time.

Next, we used the elevated plus maze paradigm to determine if iTDP-43^{A315T} mice show changes in anxiety behavior. In comparison to non-transgenic and single transgenic pTRE-TDP-43^{A315T}(13) and mThy1.2-tTA(6) controls, iTDP-43^{A315T} mice spent at 1 month threefold, and at 3 months of age fivefold more time in the open area (Fig. 2g), suggesting reduced anxiety or disinhibition. The distance each mouse travelled during trials was comparable for 1-month-old mice [5.7 ± 0.5 m (non-tg), 4.7 ± 0.5 m (ctr), 5.3 ± 1.6 m (iTDP-43^{A315T})], and only slightly reduced for 3-month-old iTDP-43^{A315T} mice [4.4 ± 0.3 m (non-tg), 4.2 ± 0.7 m (ctr), 3.7 ± 0.4 m (iTDP-43^{A315T})], suggesting that the observed deficits were rather not due to motor deficits. Taken together, constitutive neuronal expression of TDP-43^{A315T} in mice resulted in progressively compromised motor performance, impaired spatial memory acquisition and retention, increased locomotor activity and disinhibition (Fig. 2h).

Progressive muscle atrophy and weakness in iTDP-43^{A315T} mice

Muscle wasting is a key feature of ALS, resulting from degeneration of upper and/or lower motor neurons. IHC of spinal cord sections revealed intensive human TDP-43 staining in anterior horn α -motor neurons of iTDP-43^{A315T}

mice, with diffuse accumulation of TDP-43^{A315T} in the cytoplasm, as shown by staining with human and total TDP-43-specific antibodies (Fig. 3a). At 4.5 months of age, we found in some iTDP-43^{A315T} α -motor neurons dense cytoplasmic TDP-43 staining, possibly resembling inclusions (Fig. 3a). Numbers of motor neurons were comparable in iTDP-43^{A315T} and control mice at 1 [37.0 ± 2.2 (non-tg), 35.6 ± 5.8 (ctr), 38.2 ± 4.2 (iTDP-43A315T)/section] and 4.5 months of age [34.4 ± 2.8 (non-tg), 31.2 ± 2.4 (ctr), 30.8 ± 2.4 (iTDP-43A315T)/section]. Nevertheless, 4.5-month-old iTDP-43^{A315T} mice presented with a 22.5 ± 5.8 % and 23.0 ± 5.7 % reduced grip strength, compared to single transgenic controls and non-transgenic littermates, respectively (Fig. 3b). Therefore, we histologically assessed the skeletal musculature in iTDP-43^{A315T} mice over time. At 1 month of age, muscles of ThyOFF6/TDP13 and single transgenic controls and non-transgenic littermates were histologically similar (Fig. 3c). However, thereafter, staining of equatorial cross section of mThy1.2-tTA(6)/pTRE-TDP-43^{A315T}(13) calf muscles showed progressive degeneration with increased numbers of small caliber fibers (Fig. 3c). Muscle fiber size distribution analysis of laminin-stained equatorial cross sections revealed comparable profiles for mThy1.2-tTA(6)/pTRE-TDP-43^{A315T}(13), single transgenic mThy1.2-tTA(6) and pTRE-TDP-43^{A315T}(13) controls and non-transgenic mice at 1 month of age (Fig. 3d). At 4.5 months of age, a significant difference in the distribution pattern with larger numbers of small caliber fibers and reduced mean fiber areas in mThy1.2-tTA(6)/pTRE-TDP-43^{A315T}(13) mice compared to controls became apparent. Taken together, human TDP-43^{A315T} expression in motor neurons resulted in progressive muscle wasting and weakness in iTDP-43^{A315T} mice.

Progressive hippocampal and cortical degeneration in iTDP-43^{A315T} mice

TDP-43^{A315T} expression caused degeneration in the hippocampus in three of our four iTDP-43^{A315T} lines [mThy1.2-tTA(6)/pTRE-TDP-43^{A315T}(6), mThy1.2-tTA(6)/pTRE-TDP-43^{A315T}(13) and mThy1.2-tTA(15)/pTRE-TDP-43^{A315T}(6)] already at 1 month of age (Fig. 1f), and delayed hippocampal degeneration in the final line [mThy1.2-tTA(15)/pTRE-TDP-43^{A315T}(13)] (Fig. 1g). Magnetic resonance imaging (MRI) of brains from 6-month-old mice showed a global forebrain atrophy in mThy1.2-tTA(6)/pTRE-TDP-43^{A315T}(13) compared to single transgenic controls, as suggested by a 21.2 ± 1.7 % reduced total brain volume (Fig. 4a). 3D reconstruction illustrates the pronounced atrophy of the hippocampus in iTDP-43^{A315T} mice, with a 48.8 ± 2.5 % reduced size compared to controls (Fig. 4b). To determine the temporal development of hippocampal degeneration, we analyzed brains from

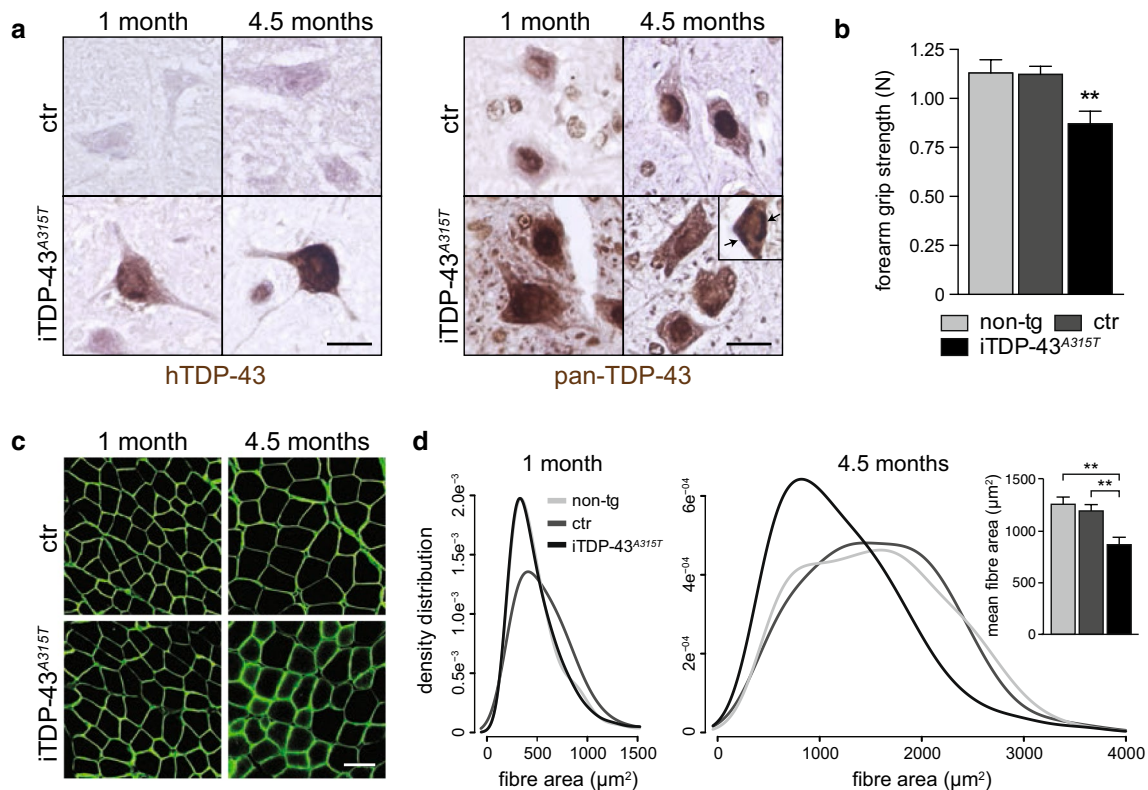


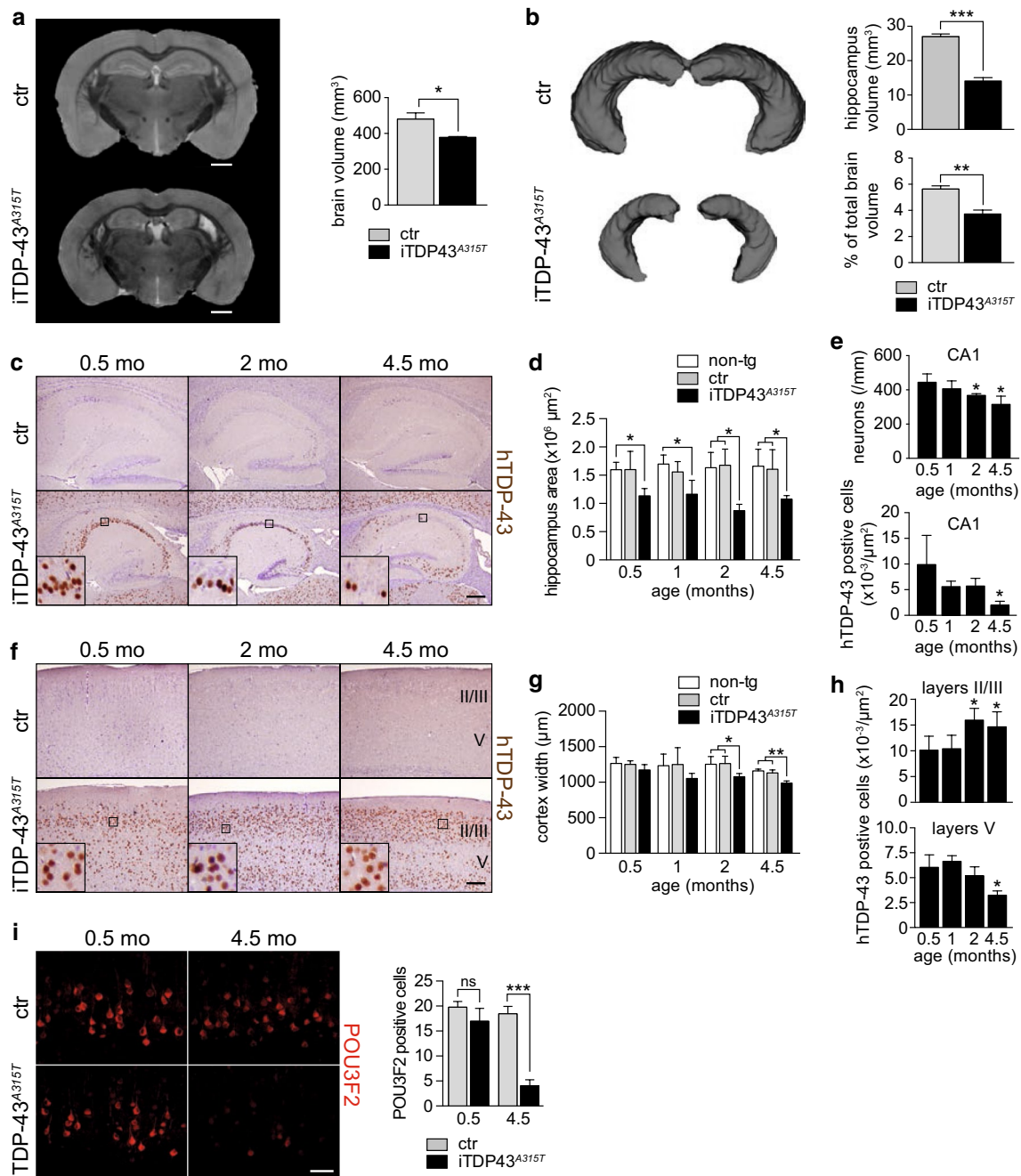
Fig. 3 Cytoplasmic TDP-43^{A315T} in spinal cord motor neurons and progressive muscle atrophy in iTDP-43^{A315T} mice. **a** Intensive staining of human TDP-43^{A315T} (hTDP-43) and total TDP-43 (pan-TDP-43) in spinal cord α -motor neurons of 1- and 4.5-month-old mThy1.2-tTA(6)/pTRE-TDP-43^{A315T}(13) iTDP-43^{A315T} mice, with cytoplasmic TDP-43 accumulation. *Inset* TDP-43 inclusions in the cytoplasm (*arrows*) of individual α -motor neuron. *Scale bars* 25 μ m. **b** Reduced grip strength in 3-month-old mThy1.2-tTA(6)/pTRE-TDP-43^{A315T}(13) iTDP-43^{A315T} mice compared to single transgenic pTRE-TDP-43^{A315T}(6) and pTRE-TDP-43^{A315T}(13) controls (ctr), and non-transgenic mice [******, $P < 0.01$, $n = 13$ (non-tg), $n = 14$ (ctr), $n = 8$ (iTDP-43^{A315T})]. **c** Basal membrane staining with laminin-specific antibodies (*green*) showed indistinguishable muscle mor-

phology in 1-month-old mThy1.2-tTA(6)/pTRE-TDP-43^{A315T}(13) iTDP-43^{A315T} and single transgenic control (ctr) mice. However, at 4.5 months iTDP-43^{A315T} muscles showed numerous small caliber and irregular fibers. *Scale bar* 50 μ m. **d** Quantification of cross sections showed comparable size distribution of muscle fibers at 1-month-old mThy1.2-tTA(6)/pTRE-TDP-43^{A315T}(13) iTDP-43^{A315T}, single transgenic pTRE-TDP-43^{A315T}(6) and pTRE-TDP-43^{A315T}(13) controls (ctr), and non-transgenic mice. However, at 4.5 months of age, muscle fiber size distribution analysis showed a left shift to smaller calibers in iTDP-43^{A315T} mice compared to single transgenic pTRE-TDP-43^{A315T}(6) and pTRE-TDP-43^{A315T}(13) controls (ctr), and non-transgenic littermates, together with a significant reduction of mean muscle fiber sizes (******, $P < 0.01$, $n = 6$)

2 weeks to 4.5 months of age. Furthermore, we extended the analysis to the cortex of iTDP-43^{A315T} mice. At 2 weeks of age already, histological analysis of brains revealed that the hippocampal structure was smaller in mThy1.2-tTA(6)/pTRE-TDP-43^{A315T}(13) mice compared to pTRE-TDP-43^{A315T}(13) littermates (Fig. 4c, d). Till 4.5 months of age, the size of the hippocampus does not decrease significantly more in iTDP-43^{A315T} mice (Fig. 4d). However, the number of TDP-43^{A315T} expressing neurons progressively reduced within the CA1 region of the hippocampus, paralleling the gradual loss of total CA1 neurons (Fig. 4e). A similar progressive degeneration of the hippocampus was found in mThy1.2-tTA(6)/pTRE-TDP-43^{A315T}(6), mThy1.2-tTA(15)/pTRE-TDP-43^{A315T}(6) and mThy1.2-tTA(15)/pTRE-TDP-43^{A315T}(13) brains, although with different temporal profiles (data not shown). Non-transgenic and mThy1.2-tTA

hippocampi were similar to pTRE-TDP-43^{A315T} littermate controls at the analyzed time points.

Different from the hippocampus, the cortical width was comparable between mThy1.2-tTA(6)/pTRE-TDP-43^{A315T}(13) and control brains at 2 weeks of age, but progressively reduced in iTDP-43^{A315T} mice over time, compared to controls (Fig. 4f, g). While numbers of TDP-43^{A315T}-expressing neurons in layer V progressively decreased, those in layers II/III of the cortex appeared to increase in iTDP-43^{A315T} brains (Fig. 4h), the latter likely due to loss of dendritic arbors of layer V neurons in layer II/III. Consistent with loss of TDP-43^{A315T}-expressing layer V neurons, the number of neurons that stained with POU3F2 [30] was reduced progressively in iTDP-43^{A315T} compared to control mice (Fig. 4i). Staining of layers II and III by POU3F2 were indistinguishable between iTDP-43^{A315T} and control



brains, consistent with absence of cell loss in these layers. Taken together, there appear to be significant differences in how distinct neuronal populations are compromised by the presence of TDP-43^{A315T} in hippocampal regions and different cortical layers, suggesting selective vulnerability.

Aberrant fragmentation, phosphorylation, ubiquitination and insolubility of TDP-43 in iTDP-43^{A315T} mice

Aberrant phosphorylation, ubiquitination, fragmentation, nuclear depletion and cytoplasmic deposition of TDP-43

are hallmarks of ALS and FTD [31]. To date, reproducing these features of the human disease in transgenic mice has been of mixed success [24]. To determine to which degree human TDP-43 neuropathology is resembled in our iTDP-43^{A315T} mice, we first extracted proteins from brains of iTDP-43^{A315T} and single transgenic control mice, using RIPA/UREA sequential extractions. We found significant amounts of human TDP-43^{A315T} in the detergent-insoluble fractions obtained from mThy1.2-tTA(6)/pTRE-TDP-43^{A315T}(13) at 2 weeks, and slightly less at 1, 4.5 and 6 months of age (Fig. 5a). Detection with pan (mouse and human)-specific TDP-43 antibodies illustrated increased

Fig. 4 Brain atrophy with neuron and synapse loss in iTDP-43^{A315T} mice. **a** Representative magnetic resonance imaging (MRI) imaging of a 6-month-old mThy1.2-tTA(6)/pTRE-TDP-43^{A315T}(13) iTDP-43^{A315T} mouse and a pTRE-TDP-43^{A315T}(13) littermate control (ctr). The total brain volume determined by MRI was reduced by $21.2 \pm 1.7\%$ in iTDP-43^{A315T} compared to ctr mice (**, $P < 0.01$, $n = 3$). **b** 3D reconstruction of the hippocampus from MRI scans and volume measurements showed marked atrophy in 6-month-old mThy1.2-tTA(6)/pTRE-TDP-43^{A315T}(13) iTDP-43^{A315T} mice compared to pTRE-TDP-43^{A315T}(13) littermate controls (ctr) (**, $P < 0.01$, $n = 3$). **c** Immunohistochemistry using a human TDP-43-specific antibody (hTDP-43, brown) of 0.5-, 2- and 4.5-month-old (mo) mThy1.2-tTA(6)/pTRE-TDP-43^{A315T}(13) iTDP-43^{A315T} mice and pTRE-TDP-43^{A315T}(13) littermate controls (ctr) showed reduced hippocampal sizes in iTDP-43^{A315T} mice, and a progressive loss of hTDP-43 positive cells in CA1 (inset). Scale bar 250 μm . **d** Area quantification revealed reduced hippocampal sizes in iTDP-43^{A315T} mice at all ages (*, $P < 0.05$, $n = 3-4$), yet no significant progression of atrophy. **e** Numbers of CA1 neurons and hTDP-43-positive transgenic cells in CA1 progressively declined in iTDP-43^{A315T} mice as they get older, as quantified for CA1 (*, $P < 0.05$, **, $P < 0.01$, $n = 3$). **f** Immunohistochemistry using a human TDP-43-specific antibody (hTDP-43, brown) of 0.5-, 2- and 4.5-month-old (mo) mThy1.2-tTA(6)/pTRE-TDP-43^{A315T}(13) iTDP-43^{A315T} mice and pTRE-TDP-43^{A315T}(13) littermate controls (ctr) showed progressive reduction of the cortical width in iTDP-43^{A315T} mice, but similar density of hTDP-43 positive cells in layers II/III (inset). Scale bar 250 μm . **g** Width measurements revealed progressive cortical atrophy as iTDP-43^{A315T} get older (*, $P < 0.05$, **, $P < 0.01$, $n = 3-4$). **h** Numbers of hTDP-43 positive transgenic cells progressively increased in cortical layers II/III and decreased in layer V in iTDP-43^{A315T} mice as they get older (*, $P < 0.05$, $n = 3$). **i** Immunofluorescence staining with the cortical layer II/III/V marker POU3F2 (red) showed similar numbers of layer V neurons at 0.5 months (mo), but a marked decrease at 4.5 mo in mThy1.2-tTA(6)/pTRE-TDP-43^{A315T}(13) iTDP-43^{A315T} mice compared to pTRE-TDP-43^{A315T}(13) littermate controls (ctr), as confirmed by quantification (***, $P < 0.001$, $n = 3-4$). Scale bar 100 μm

levels of TDP-43 in the detergent-soluble fractions of iTDP-43^{A315T} compared to control extracts, though detergent-insoluble TDP-43 was only detected in iTDP-43^{A315T} mice at 2 weeks of age, likely due to the sensitivity of the antibody (Fig. 5a). Hence, the majority of TDP-43 (human and endogenous) was solubilized in detergent-containing buffers from both iTDP-43^{A315T} and single transgenic control mice. Similar patterns of detergent-insoluble TDP-43 were found in mThy1.2-tTA(6)/pTRE-TDP-43^{A315T}(6), mThy1.2-tTA(15)/pTRE-TDP-43^{A315T}(6) and mThy1.2-tTA(15)/pTRE-TDP-43^{A315T}(13) brains (data not shown). When over-exposing membranes detected with human TDP-43-specific antibodies, we found several lower molecular weight bands in the detergent-insoluble fractions. This included TDP-43 fragments of approximately 35, 20 and 15 kDa, though much less abundant compared to the full-length protein (Fig. 5a). Interestingly, detection of TDP-43 phosphorylated at serine 409/410 revealed that the insoluble fragments are highly phosphorylated, while only some phosphorylation of the full-length protein was detectable at ~45 kDa (Fig. 5a). Interestingly, the 35 and 15 kDa

fragments were most prominently phosphorylated at 2 weeks of age, while phosphorylation of the 20 kDa fragment was only detectable at 1 month of age and increased thereafter.

Next, we used sequential extractions of cytosolic and nuclear proteins to determine cytosolic TDP-43 levels. We found low levels of hTDP-43 in the cytoplasm of iTDP-43^{A315T} brains at all ages analyzed (Fig. 5b). Detection with a pan-specific TDP-43 antibody revealed that cytoplasmic TDP-43 is most abundant in iTDP-43^{A315T} brains at 2 weeks of age, and decreases thereafter. No cytosolic TDP-43 was detectable in preparations from single transgenic control mice. Detection of nuclear H2AX and non-nuclear Grp78 confirmed separation of nuclei and cytoplasm.

Finally, we determined protein ubiquitination in detergent-soluble and -insoluble brain extracts of iTDP-43^{A315T} and control mice of different ages, and by immunohistochemistry. We found ubiquitin-positive bands in the detergent-insoluble fractions at 4.5 and more so 6-month-old iTDP-43^{A315T} mice, while band intensities in younger iTDP-43^{A315T} mice were comparable to controls (Fig. 5c). Immunoprecipitation with a human TDP-43-specific antibody followed by detection for ubiquitin showed ubiquitination of human TDP-43 in iTDP-43^{A315T} mice at 6 months of age (Fig. 5d). Consistent with the finding of progressively increasing ubiquitination, virtually no ubiquitin staining was found in brains of young iTDP-43^{A315T} mice, while at 4.5 months of age neurons in the cortex showed mostly nuclear ubiquitin staining, and eventually comprised both nucleus and cytoplasm of neurons at 6 months of age (Fig. 5e). No comparable staining was observed in control littermate brains across ages. Taken together, expression of human TDP-43^{A315T} results in its insolubility, fragmentation and aberrant phosphorylation and ubiquitination of TDP-43^{A315T} in iTDP-43^{A315T} mice.

Pronounced glial response in the cortex of iTDP-43^{A315T} mice

We next assessed the glial response during progressive cortical degeneration induced by TDP-43^{A315T} expression. Astroglial activation was determined by the presence and morphology of GFAP-positive cells in cortical layers of the motor cortex. In single transgenic control littermate brains, GFAP-positive astrocytes are mainly found in the corpus callosum and rarely in the neuronal layers of the cortex (Fig. 6a). Furthermore, their slim morphology suggests resting state astrocytes. In stark contrast, we found large numbers of tufted enlarged GFAP-positive astrocytes in all neuronal layers of the cortex of iTDP-43^{A315T} mice already at 1 month of age (Fig. 6a, b). This activation persisted over time together

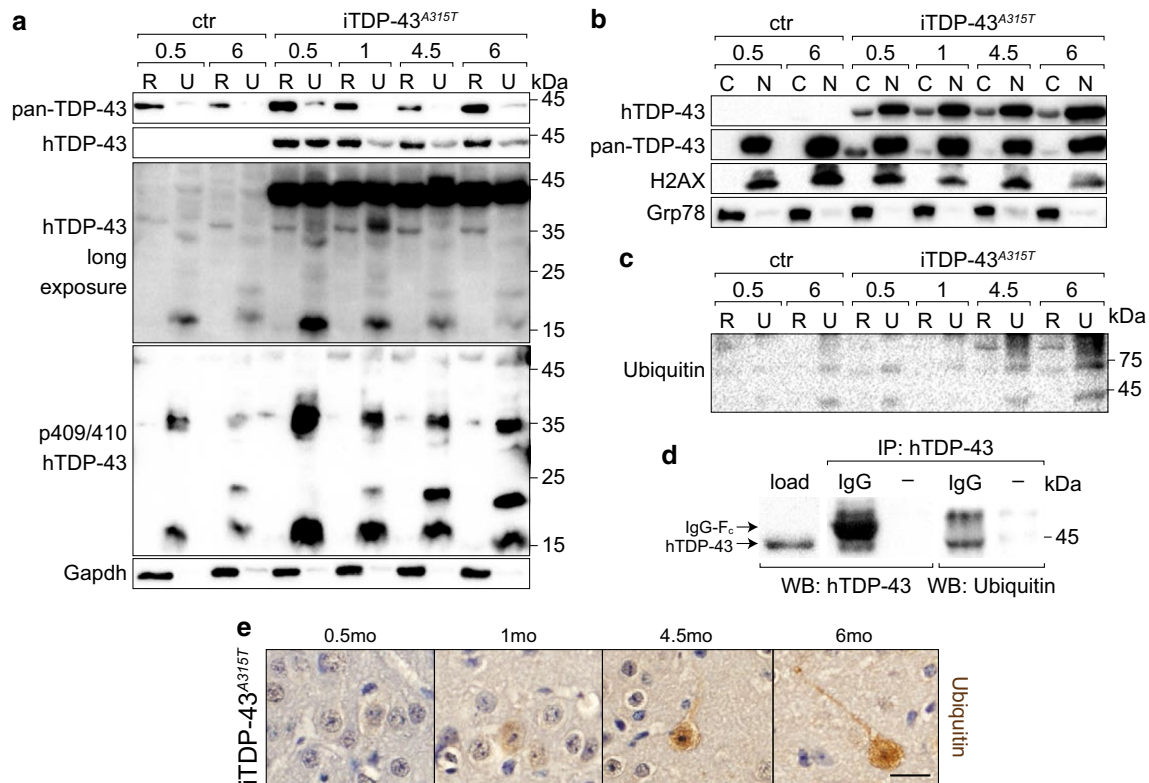


Fig. 5 Aberrant ubiquitination and insolubility of TDP-43 in iTDP-43^{A315T} mice. **a** Western blots of sequential brain extracts with RIPA (R) and urea (U) buffers showed human TDP-43 (hTDP-43) in RIPA-soluble and RIPA-insoluble (urea) fractions of mThy1.2-tTA(6)/pTRE-TDP-43^{A315T}(13) iTDP-43^{A315T}, but not single-transgenic pTRE-TDP-43^{A315T}(13) mice. Detection for total (mouse and human) TDP-43 (pan-TDP-43) revealed hTDP-43 in RIPA-soluble fractions in single-transgenic pTRE-TDP-43^{A315T}(13) mice, and in RIPA-soluble and RIPA-insoluble (urea) fractions of iTDP-43^{A315T} mice. Long exposure of blots detected with hTDP-43 revealed fragments (~35, 20 and 15 kDa) in RIPA-insoluble (urea) fractions. Antibodies specific to TDP-43 phosphorylated at Serine 409/410 (p409/410 hTDP-43) showed marked phosphorylation of TDP-43 fragments, and to a lesser degree of intact TDP-43. Gapdh confirmed equal loading. **b** Nuclear (N) and cytosol (C) extraction of iTDP-43^{A315T} and pTRE-TDP-43^{A315T}(13) brains demonstrated human TDP-43 (hTDP-43)

predominantly in nuclear, but also in cytoplasmic fractions in iTDP-43^{A315T} mice. Detection for total (mouse and human) TDP-43 (pan-TDP-43) revealed more cytoplasmic TDP-43 at 2 weeks than at 1, 4.5 and 6 months of age in iTDP-43^{A315T} mice. Nuclear H2AX and non-nuclear Grp78 confirmed extraction purity. **c** Detection of RIPA (R) and urea (U) extracts from iTDP-43^{A315T} and pTRE-TDP-43^{A315T}(13) brains showed increased protein ubiquitination at 4.5 and 6 months of age in iTDP-43^{A315T} mice. **d** Immunoprecipitation of human TDP-43 (hTDP-43) from 6-month-old iTDP-43^{A315T} brains confirmed ubiquitination of TDP-43. **e** Consistent with progressive ubiquitination in aging iTDP-43^{A315T} mice, IHC with antibodies to ubiquitin revealed faint staining of neurons (brown) at 1, more intense staining at 4.5, and intense pan-neuronal staining at 6 months of age. No staining occurred in single transgenic control and non-transgenic mice across ages (not shown). Scale bar 50 μ m

with progressive thinning of the cortex. High-resolution analysis showed GFAP-positive tufted astrocytes in close proximity to TDP-43^{A315T}-expressing neurons, suggesting activation due to ongoing pathological cellular processes (Fig. 6c).

In contrast to the pronounced activation of astrocytes together with progressive degeneration of the cortex and hippocampus, we did not find indication of microglial involvement in the process. Accordingly, staining with microglial markers IBA-1 were indistinguishable between of iTDP-43^{A315T} and control mice across ages (Supplementary Fig. 2). Taken together, neuronal expression of TDP-43^{A315T} results in a substantial and persisting activation of astrocytes.

Alleviated functional deficits upon short-term suppression of transgene expression in iTDP-43^{A315T} mice

Functional deficits in iTDP-43^{A315T} mice may result from degeneration of distinct brain regions, such as the hippocampus and/or dysfunction of neurons harboring pathological TDP-43. To test this, we switched off TDP-43^{A315T} expression for just 1 week in 3-month-old iTDP-43^{A315T} mice, by feeding a doxycycline-containing diet, to clear soluble TDP-43^{A315T} from neurons and prevent its de novo synthesis before subjecting them to the elevated plus maze, Morris water maze, open field and Rota-Rod paradigms. Directly after completion of the functional tests, all mice

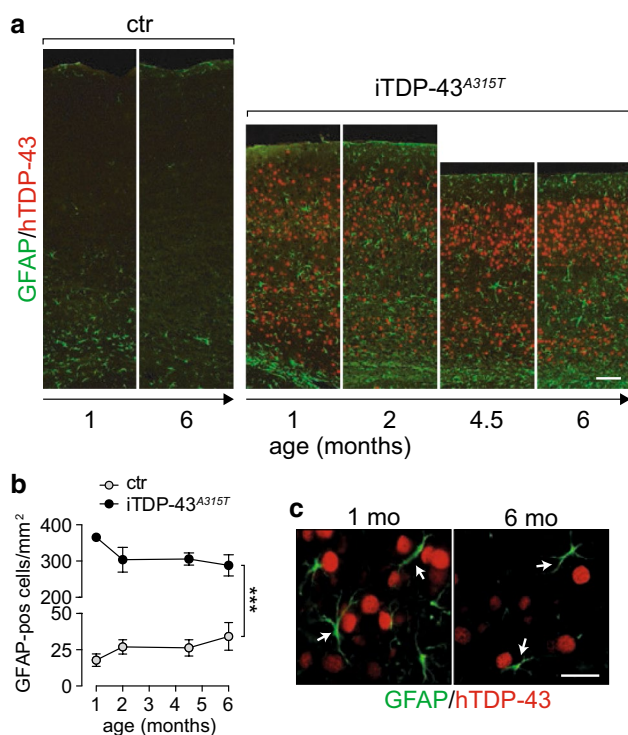


Fig. 6 Persisting reactive astrocytosis in iTDP-43^{A315T} mice. **a** Double immunofluorescence staining with antibodies to GFAP (green) and human TDP-43 (hTDP-43, red), revealed high numbers of GFAP-positive throughout all neuronal layers of the cortex in mThy1.2-tTA(6)/pTRE-TDP-43^{A315T}(13) iTDP-43^{A315T} mice, already at 1 and persisting until 6 months of age. GFAP-positive astrocytes are mostly confined to the corpus callosum in single-transgenic pTRE-TDP-43^{A315T}(13) mice. Scale bar 200 μ m. **b** Quantification confirmed very high numbers of GFAP-positive in the cortex of iTDP-43^{A315T} compared to pTRE-TDP-43^{A315T}(13) mice (***, $P < 0.001$, $n = 3$). **c** High-resolution pictures show the typical tufted appearance of reactive GFAP-positive astrocytes (arrows) in the proximity of transgenic human TDP-43^{A315T} expressing (hTDP-43, red) neurons in iTDP-43^{A315T} mice. No tufted astrocytes were found in controls (not shown). Scale bar 50 μ m

were euthanized for tissue collection. Western blot analysis of brain extracts and immunofluorescence staining showed that short-term administration of doxycycline is sufficient to suppress transgene expression completely, and allow neurons to clear virtually all human TDP-43^{A315T} (Fig. 7a, b). As expected, histological analysis of brains illustrated virtual absence of human TDP-43^{A315T}, but a comparable degree of brain atrophy (325 (untreated) vs. 319 (dox-treated) CA1 neurons/mm) in untreated and doxycycline-treated iTDP-43^{A315T} mice (Fig. 7c). However, immunofluorescence staining showed that the pronounced astrogliosis in the cortex of iTDP-43^{A315T} mice was reversed upon suppression of human TDP-43^{A315T} expression (Fig. 7d).

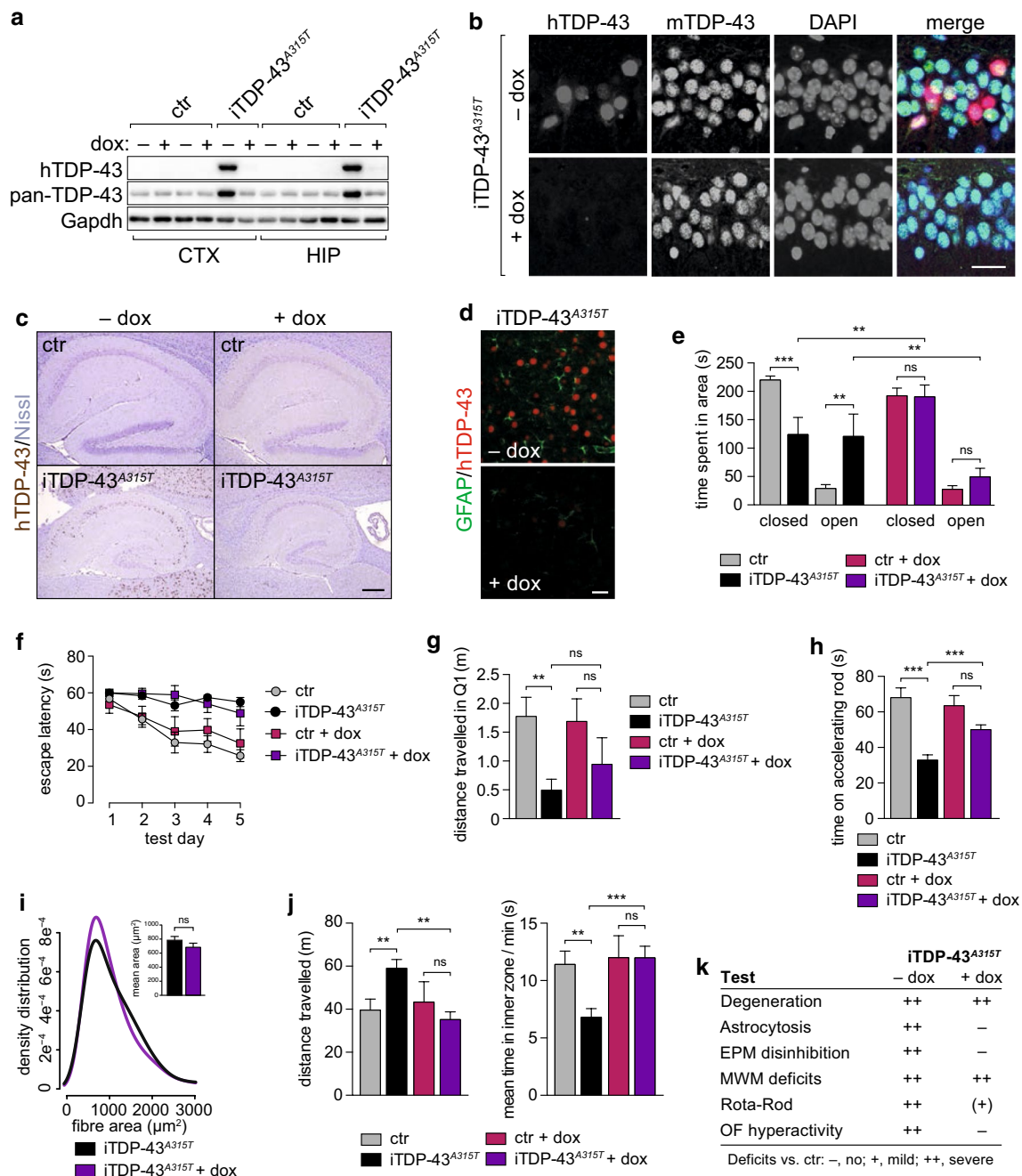
The functional analysis showed that while untreated iTDP-43^{A315T} mice spent significantly more time in the open arms of the elevated plus maze compared to single

transgenic pTRE-TDP-43^{A315T}(13) and mThy1.2-tTA(6) controls, in doxycycline-treated iTDP-43^{A315T} and control mice there is no longer a significant difference (Fig. 7e). In contrast, memory acquisition of doxycycline-treated iTDP-43^{A315T} mice in the Morris water mice was not different from untreated iTDP-43^{A315T} mice (Fig. 7f), and deficits in the probe trial presented by untreated iTDP-43^{A315T} mice persisted in doxycycline-treated iTDP-43^{A315T} mice, although the difference reached no longer significance compared to controls (Fig. 7g). Doxycycline-treated iTDP-43^{A315T} mice managed to stay 56.3 ± 5.9 % ($p < 0.001$, $n = 7$) longer on the accelerating Rota-Rod than untreated iTDP-43^{A315T} mice (Fig. 7h), despite persisting muscle atrophy (Fig. 7i). Finally, the hyperactive phenotype presented by iTDP-43^{A315T} mice in the open field, with increased travel distance and compromised exploratory patterns, was no longer present in doxycycline-treated iTDP-43^{A315T} mice (Fig. 7j). Taken together, short-term suppression of transgene expression resulted in removal of virtually all human TDP-43^{A315T} from neurons, and improved behavioral and motor functions, but persisting memory deficits and brain/muscle atrophy in iTDP-43^{A315T} mice (Fig. 7k).

Discussion

In the current study, we present novel human A315T mutant TDP-43-expressing iTDP-43^{A315T} lines with controllable transgene expression. iTDP-43^{A315T} mice were characterized by early-onset hippocampal and cortical atrophy, associated with loss of human TDP-43^{A315T}-expressing neurons and reactive astrogliosis. We found cytoplasmic localization of TDP-43 as well as detergent-insoluble TDP-43 together with the appearance of phosphorylated TDP-43 fragments and increased ubiquitination in iTDP-43^{A315T} brains. This compares to phosphorylation of TDP-43 fragments, as well as aberrant ubiquitination of TDP-43, reported in both FTLD-TDP and ALS [15, 22, 31]. Functionally, iTDP-43^{A315T} mice present with progressive memory deficits, hyperactivity, disinhibition and motor impairments. The latter were associated with TDP-43^{A315T} expression and deposition in spinal cord α -motor neurons.

TDP-43 levels in our iTDP-43^{A315T} mice were approximately 1.5- to 2-fold over endogenous levels at 4 weeks of age, and progressively increased thereafter. In neurons that expressed human mutant TDP-43^{A315T}, endogenous mouse TDP-43 expression was suppressed below detection limits, suggesting stringent control mechanisms of TDP-43 levels. Levels of transgenic TDP-43 markedly differ in previously reported lines, with some expressing up to ninefold over endogenous levels [21, 46]. For example, Igaz and colleagues directly compared expression of non-mutant TDP-43 and an NLS deletion variant (TDP-43- Δ NLS) using



the same inducible system [21]. While non-mutant TDP-43 was expressed at low levels (0.4- to 1.7-fold of endogenous) associated with a slow progression of neuron loss, TDP-43- Δ NLS reached 8- to 9-fold endogenous levels and similarly rapid hippocampal degeneration as in iTDP-43^{A315T} mice. No reduced survival was reported for these lines [21], as in our iTDP-43^{A315T} mice that have been aged over 15 months. However, early death has been reported in several TDP-43 transgenic lines [5, 37, 45, 46], often associated with very high expression levels [46], particularly in the spinal cord [37]. Apart from expression levels, the

differences in survival between TDP-43 transgenic lines may further be attributed to different promoters used for expression [21, 37, 46], or genetic backgrounds used [5]. Furthermore, reduced survival of mutant TDP-43 transgenic mice driven by the prion promoter has been linked to bowel paralysis [11, 14, 16].

In 3 of the 4 iTDP-43^{A315T} lines presented here, human TDP-43^{A315T} expression in neurons of the hippocampus results in an atrophy that is already apparent 14 days after birth, which was the youngest age analyzed. While there is no significant reduction in the size after 1 month

Fig. 7 Short-term suppression of transgenic TDP-43^{A315T} expression reduced reactive astrogliosis and improved motor, memory and behavioral deficits of iTDP-43^{A315T} mice. **a** 3-month-old mThy1.2-tTA(6)/pTRE-TDP-43^{A315T}(13) iTDP-43^{A315T} and single transgenic control mice were treated for 7 days with doxycycline. Western blotting showed virtually complete absence of human TDP-43A315T from cortical and hippocampal brain extracts of doxycycline-treated iTDP-43^{A315T} mice, resulting in control-like total levels of total TDP-43 (pan-TDP-43). Detection of Gapdh confirmed equal loading. **b** Double immunofluorescence staining confirmed absence of transgenic human TDP-43^{A315T} (hTDP-43, red) in doxycycline-treated (+dox) iTDP-43^{A315T} mice, and re-expression of mouse TDP-43 (mTDP-43, green) in all neurons, as compared to untreated (–dox) iTDP-43^{A315T} mice. Nuclei were stained with DAPI (blue). Scale bar 50 μm. **c** Hippocampal atrophy was comparable in untreated (–dox) and doxycycline-treated (+dox) iTDP-43^{A315T} mice, with absence of human TDP-43 (hTDP-43) staining in the latter. Scale bar 250 μm. **d** Immunofluorescence staining showed reduction of GFAP-positive astrocytes (green) together with reduction of human TDP-43 (hTDP-43, red) in the cortex of doxycycline-treated (+dox) compared to untreated (–dox) iTDP-43^{A315T} mice. Scale bar 50 μm. **e** Elevated plus maze: While untreated (–dox) iTDP-43^{A315T} mice spent significantly less time in the closed and more time in the open arms of the EPM compared to single transgenic controls (ctr), there were no longer significant differences between doxycycline-treated (+dox) iTDP-43^{A315T} and ctr mice [***, $P < 0.001$, **, $P < 0.01$, $n = 9$ (dox-treated ctr and iTDP-43^{A315T})]. For all functional assessments (**e–h**), dox-treated mice were compared to untreated ctr and iTDP-43^{A315T} with constitutive transgene expression presented in Fig. 2. **f** Morris water maze: memory acquisition indicated by the latency to find the submerged platform was similarly impaired in untreated (–dox) and doxycycline-treated (+dox) iTDP-43^{A315T} mice, compared to single transgenic controls (ctr). **g** However, the impairments were no longer significant in doxycycline-treated (+dox) iTDP-43^{A315T} mice in the probe trial, which was different from untreated (–dox) iTDP-43^{A315T} mice [**, $P < 0.01$, $n = 7$ (dox-treated ctr and iTDP-43^{A315T})]. **h** Accelerating Rota-Rod: motor deficits were improved in doxycycline-treated (+dox) compared to untreated (–dox) iTDP-43^{A315T} mice [***, $P < 0.001$, $n = 7$ (dox-treated ctr and iTDP-43^{A315T})]. **i** Open field: distance travelled and time in the inner zone reverted back to control (ctr) levels in doxycycline-treated (+dox) iTDP-43^{A315T} mice, different from the pronounced deficits of untreated (–dox) iTDP-43^{A315T} mice [**, $P < 0.01$, ***, $P < 0.001$, $n = 7$ (dox-treated ctr and iTDP-43^{A315T})].

of age, human TDP-43^{A315T}-expressing neurons continued to be lost thereafter. The final line, mThy1.2-tTA(15)/pTRE-TDP-43^{A315T}(13) eventually showed hippocampal atrophy after 2 months of age. This early-onset atrophy is comparable to that becoming overt 24 and 5 days after birth in reported transgenic lines with inducible expression of non-mutant human TDP-43 or M337V mutant human TDP-43, respectively [5, 8]. Other inducible TDP-43 lines expressing non-mutant or a ΔNLS variant presented with hippocampal degeneration at 3 and 1 month of age, respectively [21]. In addition to neuronal loss in the hippocampus, developmental alterations may also contribute to the hippocampal changes. However, normal hippocampal size at 1 month of age in mThy1.2-tTA(15)/pTRE-TDP-43^{A315T}(13) mice and less rapid degeneration than in the other iTDP-43^{A315T} mice, suggests that loss of neurons

rather than defective neurogenesis contribute to the morphological changes. Comparable staining of cells with the neuronal precursor marker doublecortin in the dentate gyrus and sub-ventricular zone of iTDP-43^{A315T}, single transgenic control and wild-type mice further supports this (data not shown).

In the cortex, layer V neurons were progressively lost in iTDP-43^{A315T} mice, other layers showed no overt loss of neurons despite widespread transgene expression. An apparent increase in numbers of TDP-43^{A315T}-expressing cells in layers II/III may be due to the loss of synapses from layer V neurons and therefore increase of cell density. Previous inducible TDP-43 mouse models also report cortical atrophy, determined by weight loss of brain tissue [5, 8, 21]. Non-mutant human TDP-43 transgenic mice showed neuronal loss of layer V cortical neurons together with reactive astrogliosis [46]. Similarly, the degeneration in the cortex of iTDP-43^{A315T} mice was paralleled by a pronounced and sustained activation of astrocytes, but not microglia throughout all cortical layers. Early-onset reactive astrogliosis has been reported in other TDP-43 transgenic mice, while microglial activation occurred only at advanced ages [38]. In other TDP-43 transgenic mouse models, however, early astrogliosis together with microglial activation has been reported [5]. Why astrocyte activation is consistently found in TDP-43 mouse lines, but onset of microgliosis varies remains to be shown, but differences in used promoters and genetic backgrounds may contribute. If astrogliosis contributes to degeneration or is a result of ongoing pathological processes induced by TDP-43^{A315T} expression remains to be shown. Here, amelioration of reactive astrogliosis after acute reduction of TDP-43^{A315T} levels suggests that the activation is rather in response to neuronal TDP-43^{A315T}-induced pathology. Reactive astrocytes in rats that express mutant TDP-43 in neurons release Lcn2, which is toxic to neurons [3], suggesting an astrocytic contribution to neurodegeneration in disease. Interestingly, induced pluripotent stem cell-derived astrocytes from TDP-43 mutation carriers showed TDP-43 mislocalization and decreased survival, yet no non-cell-autonomous effects on co-cultured neurons [36]. Taken together, loss of hippocampal, cortical layer V, but not layer II/III neurons in iTDP-43^{A315T} mice indicates differential vulnerability of hippocampal and cortical neurons to transgenic TDP-43 expression.

Human TDP-43^{A315T} expression and brain atrophy in iTDP-43^{A315T} mice was associated with progressive functional deficits in different behavioral and motor test paradigms. Accordingly, 1-month-old iTDP-43^{A315T} mice presented without motor impairments and only mild behavioral deficits in the elevated plus maze, while memory was already significantly compromised. However, at 3 months of age their memory acquisition became even worse in the Morris water maze, their motor performance impaired

on the Rota-Rod, they were hyperactive in the open field, showed more reduced anxiety or disinhibition on the elevated plus maze and presented with reduced grip strength and muscle atrophy. In particular, the functional motor impairments and the muscular deficits associated with TDP-43^{A315T} expression in spinal cord α -motor neurons relate to the clinical presentation of ALS. The behavioral changes, including disinhibition, stereotypic behavior and executive deficits, on the other hand, are main clinical features of behavioral variant FTD (bvFTD), which is associated with TDP-43 neuropathology in approximately 30 % of cases [6, 35]. Disinhibition in the elevated plus maze and hyperactivity with compromised exploration strategy in the open field as displayed by iTDP-43^{A315T} mice may resemble similarities to the clinical features of bvFTD. However, direct comparison of functional deficits between mouse models and human disease should be made carefully, and may rather reflect surrogate readout of functionally compromised neurons [24]. Earlier mutant human TDP-43 transgenic mice and rats present with memory deficits [1, 38, 39], similar to those seen in our iTDP-43^{A315T} mice with severe hippocampal atrophy. Memory deficits in bvFTD can be as severe as in AD [12, 18], and may present with hippocampal atrophy as in AD [19]. This hippocampal atrophy is predominantly in bvFTD with TDP-43 neuropathology [19]. Furthermore, TDP-43 pathology is found in 57 % of AD cases [27], 46 % of individuals with age-related dementia [47], and TDP-43 may contribute to memory deficits in mild cognitive impairment (MCI) and AD via the NF- κ B pathway [32]. In summary, rather than being a pure ALS or FTD model, iTDP-43^{A315T} mice model aspects of the clinical presentations of the ALS-FTD disease continuum in humans [24].

Interestingly, we found a partial recovery of functional deficits when suppressing de novo TDP-43^{A315T} synthesis for only 1 week, despite marked neurodegeneration and muscle atrophy. One explanation for the improvements after suppressing TDP-43^{A315T} expression is that the presence of aberrant TDP-43 inhibits the regenerative competence of compromised neurons. Alternatively, aberrant TDP-43 directly interferes with functional processes required for their proper function. In both cases, removing transgenic TDP-43 allows the remaining neurons to increase functionality and compensate for lost function. Recovery of endogenous murine TDP-43 expression after switching off human TDP-43^{A315T} expression may contribute to functional improvements. The failure of iTDP-43^{A315T} mice to improve memory deficits and the limited capacity to rescue impaired motor functions after switching off transgenic TDP-43^{A315T} expression is likely due to the already advanced atrophy of the hippocampus and musculature at the time treatment commenced. Conversely, the marked reversal of disinhibition/reduced

anxiety in the elevated plus maze and hyperactivity in the open field suggests that these deficits result rather from function impairment of neurons by iTDP-43^{A315T} rather than neurodegeneration. Similarly, short-term suppression of transgenic expression of a TDP-43 variant that was artificially located to the cytoplasm by deleting the nuclear localization sequence (Δ NLS) resulted in reversal of distinct functional deficits in young mice [1]. Once neurodegeneration was overt, suppression of transgenic TDP-43 Δ NLS expression did not improve functional deficits [1]. Similarly, memory deficits in our iTDP-43^{A315T} mice did not recover when transgenic TDP-43 was removed. Consistent with improved motor performance of iTDP-43^{A315T} mice after TDP-43 suppression, partial recovery of muscle function over time following switching off transgenic TDP-43 expression has previously been reported in rats [20]. A new inducible Δ NLS-TDP-43 mouse model with brain atrophy and motor impairments, published during the revision of our study, presented early death that was prevented by suppression of transgene expression [44]. In summary, our data support that even at advanced stages of degeneration, reducing pathological TDP-43 could be therapeutically beneficial. This may encourage the development of TDP-43-targeted treatments.

Taken together, we developed a novel transgenic mouse model that replicates aspects of human FTLTDP and ALS. Pronounced brain atrophy was accompanied by functional deficits that were partially reversible by acute reduction of TDP-43^{A315T} using the doxycycline-suppressible promoter system. This suggests that functional deficits are mediated at least in part directly by the presence of aberrant TDP-43. Therefore, iTDP-43^{A315T} mice are a suitable platform for investigating molecular disease mechanisms. Furthermore, the inducible transgene expression system allows for different temporal scenarios of TDP-43^{A315T} expression; for example, future studies should investigate iTDP-43^{A315T} mice in which transgene expression was suppressed until after weaning to allow brain maturation before the transgene is expressed [24]. Similar studies in other inducible TDP-43 transgenic lines have shown differences in neuropathology when the transgene was activated in the adult brain, warranting further studies [1, 5].

Acknowledgments The authors like to thank the staff of the Biological Resources Centre Wallace Wurth for animal care. We also thank Prof Virginia Lee for anti mouse TDP-43 antibodies. This work has been supported by the National Health & Medical Research Council (NHMRC; #1081916, #1020562), the NHMRC Forefront Program grant (#1037746) and the Australian Research Council (ARC; #DP1096674, #DP130102027), Motor Neuron Disease Australia and the University of New South Wales. Y.D.K. is an ARC DECRA fellow (DE130101591). G.M.H. is an NHMRC Senior Principal Research

Fellow (#1079679). L.M.I. is an NHMRC Senior Research Fellow (#1003083).

Compliance with ethical standards

Conflict of interest The authors declare no competing financial interest.

References

- Alfieri JA, Pino NS, Igaz LM (2014) Reversible behavioral phenotypes in a conditional mouse model of TDP-43 proteinopathies. *J Neurosci* 34:15244–15259. doi:10.1523/JNEUROSCI.1918-14.2014
- Baker M, Mackenzie IR, Pickering-Brown SM, Gass J, Rademakers R, Lindholm C, Snowden J, Adamson J, Sadovnick AD, Rollinson S et al (2006) Mutations in progranulin cause tau-negative frontotemporal dementia linked to chromosome 17. *Nature* 442:916–919
- Bi F, Huang C, Tong J, Qiu G, Huang B, Wu Q, Li F, Xu Z, Bowser R, Xia XG et al (2013) Reactive astrocytes secrete Icn2 to promote neuron death. *Proc Natl Acad Sci USA* 110:4069–4074. doi:10.1073/pnas.1218497110
- Buratti E, Baralle FE (2001) Characterization and functional implications of the RNA binding properties of nuclear factor TDP-43, a novel splicing regulator of CFTR exon 9. *J Biol Chem* 276:36337–36343. doi:10.1074/jbc.M104236200
- Cannon A, Yang B, Knight J, Farnham IM, Zhang Y, Wuertz CA, D'Alton S, Lin WL, Castaneda-Casey M, Rousseau L et al (2012) Neuronal sensitivity to TDP-43 overexpression is dependent on timing of induction. *Acta Neuropathol* 123:807–823. doi:10.1007/s00401-012-0979-3
- Chare L, Hodges JR, Leyton CE, McGinley C, Tan RH, Kril JJ, Halliday GM (2014) New criteria for frontotemporal dementia syndromes: clinical and pathological diagnostic implications. *J Neurol Neurosurg Psychiatry* 85:865–870. doi:10.1136/jnnp-2013-306948
- Cruts M, Gijselinck I, van der Zee J, Engelborghs S, Wils H, Pirici D, Rademakers R, Vandenbergh R, Dermaut B, Martin JJ et al (2006) Null mutations in progranulin cause ubiquitin-positive frontotemporal dementia linked to chromosome 17q21. *Nature* 442:920–924
- D'Alton S, Alshuler M, Cannon A, Dickson DW, Petrucelli L, Lewis J (2014) Divergent phenotypes in mutant TDP-43 transgenic mice highlight potential confounds in TDP-43 transgenic modeling. *PLoS One* 9:e86513. doi:10.1371/journal.pone.0086513
- DeJesus-Hernandez M, Mackenzie IR, Boeve BF, Boxer AL, Baker M, Rutherford NJ, Nicholson AM, Finch NA, Flynn H, Adamson J et al (2011) Expanded GGGGCC hexanucleotide repeat in noncoding region of C9ORF72 causes chromosome 9p-linked FTD and ALS. *Neuron* 72:245–256. doi:10.1016/j.neuron.2011.09.011
- Delerue F, White M, Ittner LM (2014) Inducible, tightly regulated and non-leaky neuronal gene expression in mice. *Transgenic Res* 23:225–233. doi:10.1007/s11248-013-9767-7
- Esmaili MA, Panahi M, Yadav S, Hennings L, Kiaei M (2013) Premature death of TDP-43 (A315T) transgenic mice due to gastrointestinal complications prior to development of full neurological symptoms of amyotrophic lateral sclerosis. *Int J Exp Pathol* 94:56–64. doi:10.1111/iep.12006
- Graham A, Davies R, Xuereb J, Halliday G, Kril J, Creasey H, Graham K, Hodges J (2005) Pathologically proven frontotemporal dementia presenting with severe amnesia. *Brain* 128:597–605. doi:10.1093/brain/awh348
- Guillemin I, Becker M, Ociepka K, Friauf E, Nothwang HG (2005) A subcellular prefractionation protocol for minute amounts of mammalian cell cultures and tissue. *Proteomics* 5:35–45. doi:10.1002/pmic.200400892
- Guo Y, Wang Q, Zhang K, An T, Shi P, Li Z, Duan W, Li C (2012) HO-1 induction in motor cortex and intestinal dysfunction in TDP-43 A315T transgenic mice. *Brain Res* 1460:88–95. doi:10.1016/j.brainres.2012.04.003
- Hasegawa M, Arai T, Nonaka T, Kametani F, Yoshida M, Hashizume Y, Beach TG, Buratti E, Baralle F, Morita M et al (2008) Phosphorylated TDP-43 in frontotemporal lobar degeneration and amyotrophic lateral sclerosis. *Ann Neurol* 64:60–70
- Hatzipetros T, Bogdanik LP, Tassinari VR, Kidd JD, Moreno AJ, Davis C, Osborne M, Austin A, Vieira FG, Lutz C et al (2014) C57BL/6 J congenic Prp-TDP43A315T mice develop progressive neurodegeneration in the myenteric plexus of the colon without exhibiting key features of ALS. *Brain Res* 1584:59–72. doi:10.1016/j.brainres.2013.10.013
- Hodges JR, Davies RR, Xuereb JH, Casey B, Broe M, Bak TH, Kril JJ, Halliday GM (2004) Clinicopathological correlates in frontotemporal dementia. *Ann Neurol* 56:399–406. doi:10.1002/ana.20203
- Hornberger M, Piguet O, Graham AJ, Nestor PJ, Hodges JR (2010) How preserved is episodic memory in behavioral variant frontotemporal dementia? *Neurology* 74:472–479. doi:10.1212/WNL.0b013e3181cef85d
- Hornberger M, Wong S, Tan R, Irish M, Piguet O, Kril J, Hodges JR, Halliday G (2012) In vivo and post-mortem memory circuit integrity in frontotemporal dementia and Alzheimer's disease. *Brain* 135:3015–3025. doi:10.1093/brain/awt239
- Huang C, Tong J, Bi F, Zhou H, Xia XG (2012) Mutant TDP-43 in motor neurons promotes the onset and progression of ALS in rats. *J Clin Invest* 122:107–118. doi:10.1172/JCI59130
- Igaz LM, Kwong LK, Lee EB, Chen-Plotkin A, Swanson E, Unger T, Malunda J, Xu Y, Winton MJ, Trojanowski JQ et al (2011) Dysregulation of the ALS-associated gene TDP-43 leads to neuronal death and degeneration in mice. *J Clin Invest* 121:726–738. doi:10.1172/JCI44867
- Inukai Y, Nonaka T, Arai T, Yoshida M, Hashizume Y, Beach TG, Buratti E, Baralle FE, Akiyama H, Hisanaga S et al (2008) Abnormal phosphorylation of Ser409/410 of TDP-43 in FTL-DU and ALS. *FEBS Lett* 582:2899–2904
- Ittner LM, Gotz J (2007) Pronuclear injection for the production of transgenic mice. *Nat Protoc* 2:1206–1215
- Ittner LM, Halliday GM, Kril JJ, Gotz J, Hodges JR, Kiernan MC (2015) FTD and ALS-translating mouse studies into clinical trials. *Nat Rev Neurol*. doi:10.1038/nrneurol.2015.65
- Ittner LM, Ke YD, Gotz J (2009) Phosphorylated tau interacts with c-Jun N-terminal kinase-interacting protein 1 (JIP1) in Alzheimer disease. *J Biol Chem* 284:20909–20916. doi:10.1074/jbc.M109.014472
- Ittner LM, Koller D, Muff R, Fischer JA, Born W (2005) The N-terminal extracellular domain 23–60 of the calcitonin receptor-like receptor in chimeras with the parathyroid hormone receptor mediates association with receptor activity-modifying protein 1. *Biochemistry* 44:5749–5754
- Josephs KA, Murray ME, Whitwell JL, Parisi JE, Petrucelli L, Jack CR, Petersen RC, Dickson DW (2014) Staging TDP-43 pathology in Alzheimer's disease. *Acta Neuropathol* 127:441–450. doi:10.1007/s00401-013-1211-9
- Kabashi E, Valdmanis PN, Dion P, Spiegelman D, McConkey BJ, Vande Velde C, Bouchard JP, Lacomblez L, Pochigaeva K, Salachas F et al (2008) TARDBP mutations in individuals with

- sporadic and familial amyotrophic lateral sclerosis. *Nat Genet* 40:572–574
29. Ling SC, Polymenidou M, Cleveland DW (2013) Converging mechanisms in ALS and FTD: disrupted RNA and protein homeostasis. *Neuron* 79:416–438. doi:10.1016/j.neuron.2013.07.033
 30. Molyneaux BJ, Arlotta P, Menezes JR, Macklis JD (2007) Neuronal subtype specification in the cerebral cortex. *Nat Rev Neurosci* 8:427–437. doi:10.1038/nrn2151
 31. Neumann M, Sampathu DM, Kwong LK, Truax AC, Micsenyi MC, Chou TT, Bruce J, Schuck T, Grossman M, Clark CM et al (2006) Ubiquitinated TDP-43 in frontotemporal lobar degeneration and amyotrophic lateral sclerosis. *Science* 314:130–133
 32. Ohta Y, Tremblay C, Schneider JA, Bennett DA, Calon F, Julien JP (2014) Interaction of transactive response DNA binding protein 43 with nuclear factor kappaB in mild cognitive impairment with episodic memory deficits. *Acta Neuropathol Commun* 2:37. doi:10.1186/2051-5960-2-37
 33. Renton AE, Majounie E, Waite A, Simon-Sanchez J, Rollinson S, Gibbs JR, Schymick JC, Laaksovirta H, van Swieten JC, Myllykangas L et al (2011) A hexanucleotide repeat expansion in C9ORF72 is the cause of chromosome 9p21-linked ALS-FTD. *Neuron* 72:257–268. doi:10.1016/j.neuron.2011.09.010
 34. Roberson ED (2012) Mouse models of frontotemporal dementia. *Ann Neurol* 72:837–849. doi:10.1002/ana.23722
 35. Rohrer JD (2011) Behavioural variant frontotemporal dementia—defining genetic and pathological subtypes. *J Mol Neurosci* 45:583–588. doi:10.1007/s12031-011-9542-2
 36. Serio A, Bilican B, Barmada SJ, Ando DM, Zhao C, Siller R, Burr K, Haghi G, Story D, Nishimura AL et al (2013) Astrocyte pathology and the absence of non-cell autonomy in an induced pluripotent stem cell model of TDP-43 proteinopathy. *Proc Natl Acad Sci USA* 110:4697–4702. doi:10.1073/pnas.1300398110
 37. Stallings NR, Puttapparthi K, Luther CM, Burns DK, Elliott JL (2010) Progressive motor weakness in transgenic mice expressing human TDP-43. *Neurobiol Dis* 40:404–414. doi:10.1016/j.nbd.2010.06.017
 38. Swarup V, Phaneuf D, Bareil C, Robertson J, Rouleau GA, Kriz J, Julien JP (2011) Pathological hallmarks of amyotrophic lateral sclerosis/frontotemporal lobar degeneration in transgenic mice produced with TDP-43 genomic fragments. *Brain* 134:2610–2626. doi:10.1093/brain/awr159
 39. Tsai KJ, Yang CH, Fang YH, Cho KH, Chien WL, Wang WT, Wu TW, Lin CP, Fu WM, Shen CK (2010) Elevated expression of TDP-43 in the forebrain of mice is sufficient to cause neurological and pathological phenotypes mimicking FTL-D-U. *J Exp Med* 207:1661–1673. doi:10.1084/jem.20092164
 40. Van Deerlin VM, Leverenz JB, Bekris LM, Bird TD, Yuan W, Elman LB, Clay D, Wood EM, Chen-Plotkin AS, Martinez-Lage M et al (2008) TARDBP mutations in amyotrophic lateral sclerosis with TDP-43 neuropathology: a genetic and histopathological analysis. *Lancet Neurol* 7:409–416
 41. van Eersel J, Ke YD, Liu X, Delerue F, Kril JJ, Gotz J, Ittner LM (2010) Sodium selenate mitigates tau pathology, neurodegeneration, and functional deficits in Alzheimer's disease models. *Proc Natl Acad Sci USA* 107:13888–13893. doi:10.1073/pnas.1009038107
 42. van Eersel J, Stevens CH, Przybyla M, Gladbach A, Stefanoska K, Chan CK, Ong WY, Hodges JR, Sutherland GT, Kril JJ et al (2015) Early-onset axonal pathology in a novel P301S-Tau transgenic mouse model of frontotemporal lobar degeneration. *Neuropathol Appl Neurobiol*. doi:10.1111/nan.12233
 43. Vanden Broeck L, Callaerts P, Dermaut B (2014) TDP-43-mediated neurodegeneration: towards a loss-of-function hypothesis? *Trends Mol Med* 20:66–71. doi:10.1016/j.molmed.2013.11.003
 44. Walker AK, Spiller KJ, Ge G, Zheng A, Xu Y, Zhou M, Tripathy K, Kwong LK, Trojanowski JQ, Lee VM (2015) Functional recovery in new mouse models of ALS/FTLD after clearance of pathological cytoplasmic TDP-43. *Acta Neuropathol*. doi:10.1007/s00401-015-1460-x
 45. Wegorzewska I, Bell S, Cairns NJ, Miller TM, Baloh RH (2009) TDP-43 mutant transgenic mice develop features of ALS and frontotemporal lobar degeneration. *Proc Natl Acad Sci USA* 106:18809–18814. doi:10.1073/pnas.0908767106
 46. Wils H, Kleinberger G, Janssens J, Pereson S, Joris G, Cuijt I, Smits V, Ceuterick-de Groote C, Van Broeckhoven C, Kumar-Singh S (2010) TDP-43 transgenic mice develop spastic paralysis and neuronal inclusions characteristic of ALS and frontotemporal lobar degeneration. *Proc Natl Acad Sci USA* 107:3858–3863. doi:10.1073/pnas.0912417107
 47. Wilson RS, Yu L, Trojanowski JQ, Chen EY, Boyle PA, Bennett DA, Schneider JA (2013) TDP-43 pathology, cognitive decline, and dementia in old age. *JAMA Neurol* 70:1418–1424. doi:10.1001/jamaneurol.2013.3961
 48. Winton MJ, Igaz LM, Wong MM, Kwong LK, Trojanowski JQ, Lee VM (2008) Disturbance of nuclear and cytoplasmic TAR DNA-binding protein (TDP-43) induces disease-like redistribution, sequestration, and aggregate formation. *J Biol Chem* 283:13302–13309